universität wien

MASTERARBEIT

Titel der Masterarbeit

„Optimization of [^{18}F]fluoride activation for microfluidic radiosynthesis“

verfasst von

Maximilian Emberger

angestrebter akademischer Grad

Master of Science (MSc)

Wien, 2015

Studienkennzahl lt. Studienblatt:	A 066 862
Studienrichtung lt. Studienblatt:	Masterstudium Chemie
Betreut von:	Assoc.-Prof. Dr. Wolfgang Wadsak

“You can never be overdressed or overeducated.”

— Oscar Wilde

Acknowledgements

First of all, I would like to thank Assoc.-Prof. Dr. Wolfgang Wadsak and Assoc.-Prof. Dr. Markus Mitterhauser for letting me be part of their working group at the Radiochemistry and Biomarker Development Unit over the course of my Master's thesis. And I especially would like to thank Assoc.-Prof. Dr. Wolfgang Wadsak for sparking my interest in this field of research, providing me with an intriguing thesis topic and being an admirable thesis supervisor.

Special thanks also go to my supervisor Dr. Cécile Philippe for teaching and supporting me throughout the whole thesis with patience and kindness, for our daily walks to get some radioactivity and for always taking the time for any questions or problems I had.

Thank you to the whole team for making working in a windowless basement always feel bright and cheerful. I would like to particularly thank my coffee companions Chrysoula, Moni, Christina and Sarah for many laughs, scientific assistance and general encouragement.

I would also like to thank Gudi, Laura, Max, Nena and Philip for making most lectures and lab courses throughout the Master's studies much more enjoyable and for bringing a sense of home to Vienna.

Last but not least, a huge thanks to my family for supporting me throughout my studies and my life.

Abstract

Aim

This thesis investigated the use of novel elution solutions for separation of cyclotron-produced [^{18}F]fluoride from water. The aim was to find an elution solution that avoids or minimizes the azeotropic drying step following the elution to activate the [^{18}F]fluoride for nucleophilic radiofluorination. A special focus was on the applicability into a microfluidic reaction system as conventional solutions cause occasional clogging of the reactors.

Methods

Elution solutions A through F were prepared with Kryptofix® 222 (58.4 µmol/ml) and potassium carbonate (32.6 µmol/ml) with acetonitrile and a water content from 0 % to 20 %. Elution solution WA contained potassium hydroxide (167 µmol/ml) and Kryptofix® 222 (250 µmol/ml) in pure acetonitrile. Tetrabutylammonium hydroxide (56.3 µmol/ml) and tetraethylammonium bicarbonate (78.4 µmol/ml) were used in 80/20 (v/v) acetonitrile and water.

Elution profiles were generated for four different columns: 30-PS-HCO_3^- (Macherey-Nagel), Sep-Pak AccelPlus QMA Plus Light (Waters) and Fluoride Trap & Release (25 mg and 9 mg sorbent; ORTG Inc.).

[^{18}F]FE@SUPPY and [^{18}F]FE@SUPPY:2 radiosyntheses were used for indicating the reactivity of eluted [^{18}F]fluoride. Dried [^{18}F]fluoride was heated with an acetonitrile precursor solution (15 mg/ml Tos@SUPPY or 20 mg/ml Tos@SUPPY:2) at 75 °C for 20 minutes and the reaction was quenched with water. Microfluidic syntheses of [^{18}F]FE@SUPPY:2 were conducted in the automated Advion NanoTek® system with 5 mg/ml Tos@SUPPY:2 in acetonitrile at temperatures from 150 – 170 °C and an overall pump rate during the reaction of 60 µl/min. Purity was determined via radio-HPLC and the radiochemical incorporation yield was determined via radio-TLC.

Results

Reducing the water content in conventional elution solutions from 20 % to 1 % only slightly impaired the elution efficiency (93.7 ± 0.0 % compared to 98.0 ± 1.5 %; column: PS-HCO_3^-; volume: 1 ml). In the same setup, solution WA eluted 98.4 ± 0.8 %, TBAH solution eluted 97.2 ± 0.6 % and TEAB solution eluted 94.4 ± 3.8 % of [^{18}F]fluoride.

Manual [^{18}F]FE@SUPPY:2 radiosynthesis with conventional conditions showed high standard deviations with 250 µl reaction volume (15.7 ± 13.5 % for azeotropic dried eluate from solution A; n=9), while at 500 µl reaction volume, only TBAH solution without azeotropic drying proved to be more efficient than standard conditions (32.8 ± 6.5 % improvement). No improved method could be found for [^{18}F]FE@SUPPY radiosyntheses.

While microfluidic radiosynthesis of [^{18}F]FE@SUPPY:2 achieved 82.2 ± 23.4 % incorporation rate under conventional conditions (solution A, 160 °C, 60 µl/min overall pump rate, azeotropic drying), use of TBAH solution increased the conversion to 97.5 ± 1.2 %.

Conclusion

Several of the investigated elution solutions sufficiently eluted [^{18}F]fluoride. In manual vessel-based radiosyntheses, no reproducible significant increase in reactivity could be achieved. In microfluidic radiosyntheses, TBAH solution increased the incorporation yield and azeotropic drying proved to be essential in all reactions.

Zusammenfassung

Ziel

Diese Arbeit beschäftigte sich mit der Anwendung neuer Elutionslösungen zur Abtrennung von im Zyklotron produzierten [^{18}F]Fluorid von Wasser. Das Ziel war es, eine Elutionslösung zu finden, welche die azeotrope Trocknung nach der Elution zum Akitivieren des [^{18}F]Fluorids für nukleophile Radiofluorinierung minimiert oder vermeidet. Ein besonderer Fokus lag auf der Anwendbarkeit für ein mikrofluides Reaktionssystem, da konventionelle Lösungen gelegentlich die Reaktoren verstopfen.

Methoden

Elutionslösungen A bis F wurden mit Kryptofix® 222 (58.4 µmol/ml) und Kaliumcarbonat (32.6 µmol/ml) mit Acetonitril und einem Wasseranteil von 0 % bis 20 % hergestellt. Elutionslösung WA enthielt Kaliumhydroxid (167 µmol/ml) und Kryptofix® 222 (250 µmol/ml) in reinem Acetonitril. Tetrabutylammoniumhydroxid (56.3 µmol/ml) und Tetraethylammoniumbicarbonat (78.4 µmol/ml) wurden in 80/20 (v/v) Acetonitril und Wasser verwendet.

Elutionsprofile wurden bei vier verschiedenen Säulen durchgeführt: 30-PS-HCO_3^- (Macherey-Nagel), Sep-Pak AccelPlus QMA Plus Light (Waters) und Fluoride Trap & Release (25 mg oder 9 mg Füllmenge; ORTG Inc.).

Radiosynthesen von [^{18}F]FE@SUPPY und [^{18}F]FE@SUPPY:2 wurden zur Bestimmung der Reaktivität des eluierten [^{18}F]Fluorids herangezogen. Getrocknetes [^{18}F]Fluorid wurde mit einer Vorläuferlösung in Acetonitril (15 mg/ml Tos@SUPPY oder 20 mg/ml Tos@SUPPY:2) bei 75 °C für 20 Minuten erhitzt und danach die Reaktion mit Wasser gestoppt. Mikrofluide Synthesen von [^{18}F]FE@SUPPY:2 wurden automatisiert im Advion NanoTek® System mit 5 mg/ml Tos@SUPPY:2 in Acetonitril bei Temperaturen von 150 – 170 °C und einer Gesamtpumpengeschwindigkeit von 60 µl/min durchgeführt. Reinheit wurde mittels radio-HPLC und der radiochemische Inkorporationsrate mittels radio-DC bestimmt.

Ergebnisse

Die Reduktion des Wasseranteils der üblich verwendeten Lösung von 20 % auf 1 % verminderte die Elutionseffizienz nur gering (93.7 ± 0.0 % verglichen mit 98.0 ± 1.5 %; Säule: PS-HCO_3^-; Volumen: 1 ml). Lösung WA eluierte in der gleichen Anordnung 98.4 ± 0.8 % [^{18}F]Fluorid, während die TBAH Lösung 97.2 ± 0.6 % und die TEAB Lösung 94.4 ± 3.8 % von der Säule entfernte. Manuelle [^{18}F]FE@SUPPY:2 Radiosynthese zeigte unter konventionellen Bedingungen hohe Standardabweichungen bei 250 µl Reaktionsvolumen (15.7 ± 13.5 % für azeotrop getrocknetes Eluat der Lösung A; n=9), während bei 500 µl Reaktionsvolumen nur TBAH Lösung ohne azeotrope Trocknung einen höhere Einbaurate als die Standardbedingungen aufwies (32.8 ± 6.5 % Verbesserung). Für [^{18}F]FE@SUPPY Radiosynthesen konnte keine verbesserte Methode gefunden werden.

Während bei der mikrofluiden Radiosynthese von [^{18}F]FE@SUPPY:2 bei konventionellen Bedingungen (Lösung A, 160 °C, 60 µl/min Gesamtpumpengeschwindigkeit, azeotrope Trockung) eine Einbaurate von 82.2 ± 23.4 % erzielt wurde, konnte mit Einsatz von TBAH Lösung diese auf 97.5 ± 1.2 % gesteigert werden.

Conclusio

Einige der untersuchten Elutionslösungen eluierten [^{18}F]Fluorid ausreichend. In den manuellen Radiosynthesen konnte keine reproduzierbare signifikante Erhöhung der Reaktivität erreicht werden. In den mikrofluiden Radiosynthesen zeigte nur die TBAH Lösung eine erhöhte Einbaurate während die azeotrope Trocknung sich in allen Reaktionen als wichtig erwies.

Contents

Figures and tables

Introduction

Nuclear chemistry and radiochemistry

Nuclear and radiochemistry is a scientific field covering a wide array of subjects. It consists of the studies of physical and chemical properties of artificially produced radioactive elements, but also the studies of fundamental principles like the nuclear structure, nuclear reactions and radioactive decay. Furthermore, it covers topics such as geochronology and cosmochemistry, the nuclear processes in the universe. Radioactivity can be utilized in a myriad of fields, for example in radioanalysis, chemistry, life sciences, industrial applications or environmental sciences. [1]

The basis for all of this is radioactive decay, a spontaneous nuclear transformation. As it has been demonstrated to be mostly insusceptible to temperature, pressure or chemical form, radioactive nuclides can be characterized by energy and mode of decay and their decay period while neglecting their physicochemical state.

Half-life ($t_{1/2}$) is the necessary time for half of the radioactive atoms in a sample to decay and characteristic for each nuclide. In practice, the measured radioactivity decreases to half of its value in that time. Half-lives can vary from fractions of seconds to millions of years [2].

Alpha decay

Alpha decay is a process in which the parent nucleus emits a helium nucleus consisting of two protons and two neutrons. Those helium nuclei are also called alpha particles and are emitted with discrete energies in the range of 4 to 10 MeV. Due to the high mass and charge of alpha particles compared to other forms of radiation they have greater ionization power but a poor ability to penetrate matter [3].

$$ {}^{A}_{Z}P \rightarrow {}^{A-4}_{Z-2}D + {}^{4}_{2}He + Q_{\alpha} $$

Scheme 1: Reaction equation of alpha decay

P denotes the parent nuclide while D identifies the daughter nuclide. The mass number A is the sum of number of protons Z and the number of neutrons N while Q denotes the energy released in the decay.

Beta decay

A nuclear decay process in which the atomic number Z changes but the mass number A remains unchanged is called beta decay. Three types of beta decay can be differentiated.

The first type is beta minus (β^-) decay in which an electron (beta minus particle) and an antineutrino are emitted from a nucleus with an excess of neutrons. The decay energy is divided between the antineutrino and the electron, resulting in a continuous energy spectrum with a characteristic maximum energy E_{max} [3].

$$ {}^{A}_{Z}P \rightarrow {}_{Z+1}{}^{A}D + e^- + \bar{\nu_e} + Q_{\beta^-} $$

Scheme 2: Reaction equation of beta minus decay

Another type of beta decay is the beta plus (β^+) decay. Here, to balance out the proton excess in the nucleus, a proton is transformed into a neutron by emission of a positron (beta plus particle) and a neutrino. The decay energy is shared between positron and neutrino and results, as with beta minus decay, in an energy spectrum for the positron with a maximum energy. This type of decay is only possible with decay energies significantly above 1.022 MeV because two electrons of opposite charge with an energy equivalence of 0.511 MeV are produced in the nucleus. While the positive electron, the positron, is emitted from the nucleus the negative electron fuses with a proton to yield a neutron.

$$ {}^{A}_{Z}P \rightarrow {}_{Z-1}{}^{A}D + e^+ + \nu_e + Q_{\beta^+} $$

Scheme 3: Reaction equation of beta plus decay

A noteworthy characteristic about positron emission amongst all types of beta decay is that the created positron can be considered the antiparticle of an electron. Therefore, if a positron comes in contact with an electron, a simultaneous annihilation of both particles occurs, converting them into energy. The result are two photons with energies equal to the rest masses of the electron or positron (0.511 MeV) emitted in opposite directions. The detection of this annihilation radiation is the basis for positron emission tomography (PET, see p. 23) [3].

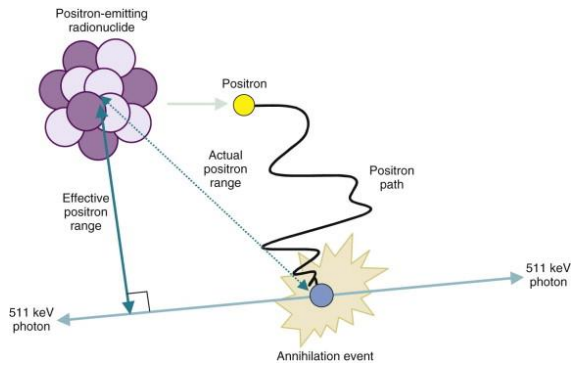

Figure 1: Beta plus decay and the following annihilation radiation (from [4])

Electron capture (EC) is the third type of beta decay and results in the same change of the nucleus as beta plus decay. This change is achieved by absorption of a proximate electron by the nucleus. Positron emission and electron capture are competing modes of decay and often occur in the same radionuclides although electron capture is predominant in nuclides with higher atomic numbers and low transition energies. At transition energies below 1.022 MeV positron emission does not occur [5].

$$ {}^{A}_{Z}P + e^{-} \rightarrow {}^{A}_{Z-1}D + \nu_e + Q_{EC} $$

Scheme 4: Reaction equation of electron capture

Gamma radiation

Gamma radiation is the result of a nuclide in an excited state, a so called nuclear isomer, reverting to a lower or ground state. In this process, an isomeric transition, gamma rays with discrete energy levels are emitted corresponding to the difference in energy levels. In contrast to all other discussed types of radiation which is of particulate nature, gamma rays are photons. Due to the fact that gamma radiation has neither resting mass nor charge it has a significantly greater penetration power and longer ranges. But gamma radiation is still absorbed and ionizes matter through the photoelectric effect [6].

Nuclear medicine and radiopharmacy

The origins of nuclear medicine trace back to only a few years after radioactivity was discovered when Marie and Pierre Curie proposed the use of radium for treating cancer in 1905 [7]. Nowadays, nuclear medicine utilizes the radiation emitted from the decay of radionuclides to either gain physiological information in patients or to therapize disease. For this, three types of radionuclides are used. Firstly, positron emitters are used for imaging with positron emission tomography (PET). Gamma emitters can be used for imaging via single photon emission computed tomography (SPECT) instead. Both types of imaging radionuclides have half-lives in the magnitude of minutes or hours. There are also therapeutic radionuclides which are mostly highly energetic β^- emitters with half-lives of several hours or days [8].

Radionuclide	Half-life	E_{max} [keV]	Radiation type	Production
Positron emitters				
^{11}C	20.3 min	961	β^+ (100%)	Accelerator
^{13}N	9.97 min	1190	β^+ (100%)	Accelerator
^{15}O	2.1 min	1732	β^+ (100%)	Accelerator
^{18}F	109.8 min	634	β^+ (97%)	Accelerator
^{68}Ga	67.6 min	1899, 770	β^+ (89%)	Generator
Gamma emitters				
^{99m}Tc	6.0 h	141	γ	Generator
^{123}I	13.3 h	159	γ	Accelerator
Therapeutic radionuclides				
^{90}Y	64.0 h	2270	β^-	Generator
^{131}I	8.0 d	1810	β^-	Fission
^{153}Sm	1.95 d	103 (280)	γ (β^-)	Reactor
^{177}Lu	6.71 d	113, 208.4 (598)	γ (β^-)	Reactor
^{186}Re	3.8 d	1100	β^-	Reactor

Table 1: Selected radionuclides used in nuclear medicine (from [8])

Radiopharmaceuticals for PET-imaging are composed of a positron emitting radionuclide and a molecular structure such as a vector, vehicle or ligand. Sometimes a linker between them is necessary to stabilize the compound. The vehicle structure has to be highly specific and selective towards a target site. Popular targets are selected receptor systems, antigens, transporters, specific metabolic

alterations such as up-regulated conditions, hypo-oxygenation of tissue, different energy demand of cells, changes in gene and protein expression, or differences in vascularization or perfusion [9].

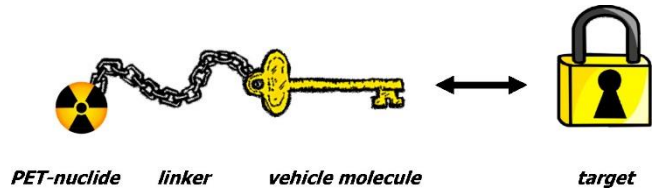

Figure 2: Schematic structure of a PET radiopharmaceutical and its interaction with a target (from [9])

Specific activity is an important parameter to consider in radiopharmaceuticals and in biodistribution of PET tracers. It is defined as the radioactivity per unit mass of a radionuclide or a labelled compound. In radiopharmaceuticals with low specific activity, non-radioactive molecules compete with their radioactive counterparts and thereby lowering the uptake of the tracer in tissues and also the specific interaction between tracer and target. High specific activity is therefore mandatory in visualizing receptor densities [10].

As PET tracer synthesis consists of working with high amounts of radioactivity substances, the radiation burden of the operator has to be minimized by shielding the synthesis apparatus with lead and by automatization of the synthesis procedure as much as possible. Furthermore, the half-life of the radionuclide for labelling has to be considered. As a rule of thumb, the total time for radiosynthesis including purification and formulation should not exceed three isotope half-lives. Thus, it can be ensured that enough radioactive tracer is available to administer for a PET scan.

To ensure a high and reliable incorporation of a radionuclide into a vehicle molecule and purification in a matter of minutes, several new technologies have been adapted: microwaves, microfluidics, ultrasound and solid-phase extraction. As only low nanomolar amounts of radionuclide are produced, precursor is usually present in such a stoichiometric excess that even lethargic reactions may take place in a matter of seconds or minutes. However, at this radionuclide concentration even small amounts of impurities in solvents and reagents may play a significant role in the reactions [11].

As synthesized tracers are pharmaceuticals intended for application in humans, certain standards for the formulated product have to be met. There are physicochemical tests where radionuclidic and radiochemical purity as well as pH, ionic strength, and osmolality of the product solution are determined. On the other hand, biological tests determine the sterility, apyrogenicity, and toxicity of the material [12].

Production of radionuclides for nuclear medicine

Cyclotron-produced radionuclides

One way to produce radionuclides with high specific activity is the bombardment of a target with an ion beam in a cyclotron. Charged particles such as protons, electrons or hydride ions are generated at the ion source located in the center of the cyclotron. The particles are accelerated in a vacuum chamber with two so called dees, semicircular metallic cylinders that are connected to high frequency alternating voltage. The apparatus is placed between the two poles of a magnet to get the magnetic field constrain the ion beam to flat circular paths. In the space between the two dees, ions are accelerated due to the potential difference between the dees causing a radius increase of the ion pathway as the energy of the ions increase. In conventional cyclotrons maximum energies of about 25 MeV for protons and deuterons and about 50 MeV for α particles are available. This high energy ion beam is then deflected onto an irradiation target [13].

Medical cyclotrons are used to produce short-lived, positron emitting radionuclides for PET-imaging. Hydride ions are commonly accelerated instead of protons as the housing of the cyclotron does not become radioactive. Furthermore, two carbon-stripping foils that strip the hydride ions of their electrons can be utilized to split the beam. Thus, two targets can be irradiated at the same time [10].

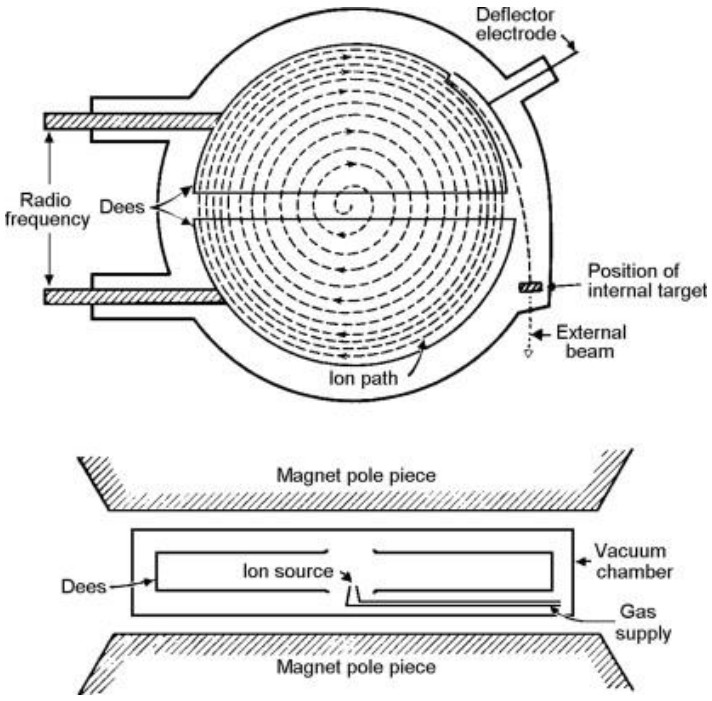

Figure 3: Principle of a cyclotron (from [13])

Generator-produced radionuclides

A generator is a simple tool to make radionuclide production for PET available for sites without a cyclotron. It utilizes the relationship of a parent-daughter radionuclide pair where the half-life of the parent nuclide is longer than that of the daughter. In this case, an equilibrium between the activities of parent and daughter is attained. If the daughter nuclide is chemically separated from its parent nuclide, a buildup of daughter product activity in the parent nuclide fraction can be observed as seen in Figure 4 [14].

These properties are exploited for generator-production of radionuclides. A parent-daughter radionuclide pair is immobilized on a matrix. Due to their different chemical properties the daughter nuclide can be extracted while leaving the parent nuclide on the matrix. The daughter nuclide replenishes and can be extracted time and time again for several radiopharmaceutical applications [15].

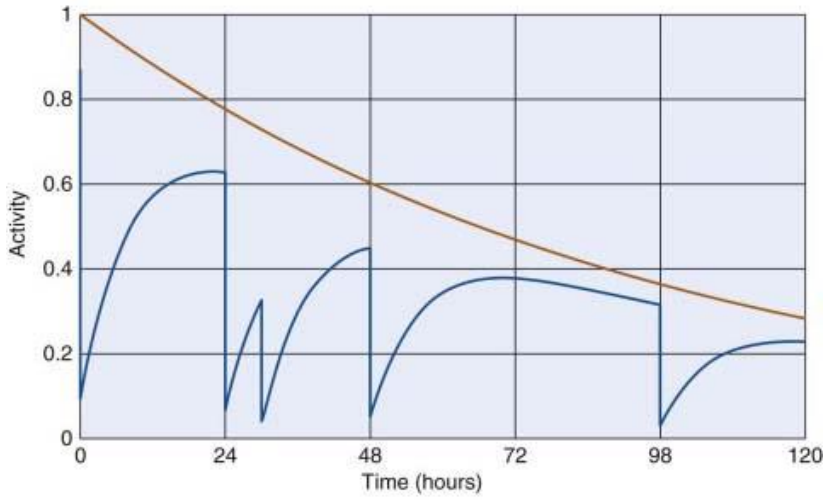

Figure 4: ^{99}Mo activity in a generator (orange), normalized to 1 at the beginning. Blue lines show the ^{99m}Tc activity available for elution, assuming 90% elution efficiency and irregular elution intervals (from [15])

Imaging in nuclear medicine

Single-photon emission computed tomography

To measure the distribution of gamma radiation emitting radiopharmaceuticals a so-called gamma camera is employed. It consists of a detector with a sodium iodide crystal connected to an array of photomultiplier tubes and is faced with a lead collimator. The detector is wired to a processing unit. The planar camera acquires a two-dimensional image of a three-dimensional distribution of the radionuclide. To acquire a three-dimensional picture, single-photon emission computed tomography (SPECT) is used. Here, the same detector rotates around a stationary patient, thus acquiring several two-dimensional images over 360°. With computer reconstruction a three-dimensional image can be created out of all two-dimensional scans [16].

Positron emission tomography

For positron emission tomography (PET), beta plus particle emitting radiotracers are employed but only the successive annihilation radiation, two 511 keV photons emitted in opposite directions, is measured. The two corresponding photons are registered simultaneously by a ring of detector units. As only coincident photons are detected, no lead collimator is needed thus increasing the detection sensitivity by a factor 10 to 100 compared to SPECT. To accommodate events at other points along the coincidence line the time window for coincidences is adjusted to approximately 6 to 12 nanoseconds. There are three main types of coincidences: True coincidences are photon pairs resulting from the same annihilation event and showing the actual position of the event. Scattered coincidences where one or two of the photons from the same annihilation are scattered before detection. Random coincidences happen when photons from two unrelated annihilation events are detected simultaneously (Figure 5).

A typical PET camera consists of a patient bed that moves slowly through the stationary detector ring. The most common detector materials are gadolinium silicate (GSO), lutetium oxyorthosilicate (LSO), or bismuth germanate (BGO) as they provide a high detection efficiency and a high signal-to-noise ratio. By reconstructing the detected signals electronically, three-dimensional imaging capability displaying transverse, sagittal and coronal image planes is provided.

As PET only provides physiological information in form of an image of the distribution of the radiotracer it can be combined with computer tomography (CT) or magnetic resonance tomography (MRT) to provide morphological information [16].

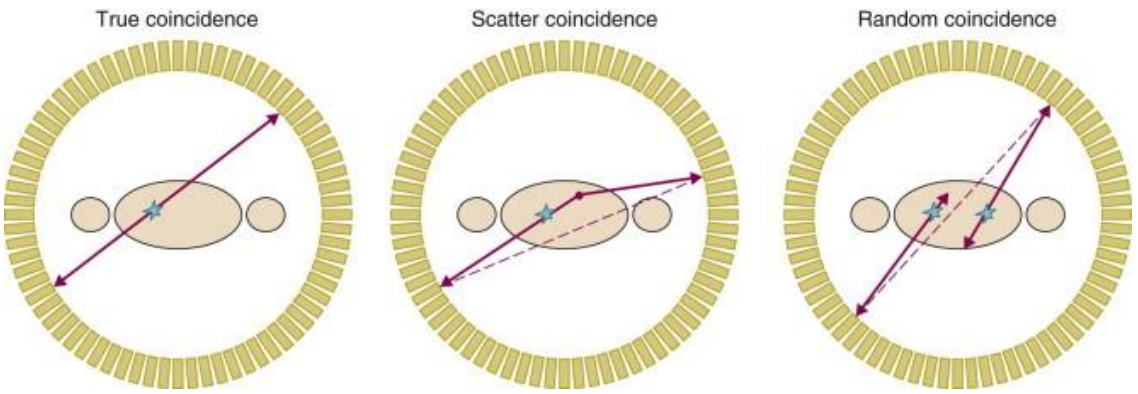

Figure 5: Coincidence events detected by PET. Scatter coincidences and random coincidences deliver wrong information and contribute background noise for the signal (from [4])

Chemistry of [^{18}F]fluorine

Electrophilic substitution as [^{18}F]F_2

For electrophilic radiofluorination, fluorine-18 is required to be generated as [^{18}F]F_2. The most common radionuclide production method is via the ^{20}Ne(d,α)^{18}F reaction by irradiation of a passivated Ni-target containing neon gas with 200 µmol F_2 as carrier.

Some major drawbacks hinder the viability of the electrophilic labelling pathway: On the one hand, fluorine-18 adsorbs to the wall which can only be minimized by addition of elemental fluorine to the target gas. On the other hand, fluorine addition lowers the specific activity of fluorine-18 [17]. Also, due to the minuscule amount of produced fluorine-18, only one fluorine atom in a molecule is radioactive and consequently only half of the tracer precursor molecules will be radioactively labelled resulting in a maximum chemical yield of 50%. To gain a more selective and less reactive fluorinating agent, [^{18}F]F_2 can be converted into acetylhypofluorite ([^{18}F]CH_3COOF) or xenon difluoride ([^{18}F]XeF_2) [18, 19]. Electrophilic fluorination offers ways to radioactively label electron-rich compounds (e.g. alkenes, aromatic molecules, carbanions, etc.) [20].

Nucleophilic substitution as [^{18}F]F^-

For nucleophilic radiofluorination, fluorine-18 is generated as [^{18}F]fluoride in aqueous solution. This is achieved with the ^{18}O (p,n) ^{18}F reaction by irradiating highly enriched ^{18}O-water with a proton beam in a cyclotron [21]. Through this way, a high specific activity is achieved which is essential for targeting low density binding sites like neuronal receptors as these have to be investigated without causing a pharmacological imbalance. As [^{18}F]fluoride has a high charge density it is strongly hydrated in water and thus inactivated for nucleophilic reactions [20].

Activation of [^{18}F]fluoride

To obtain reactive [^{18}F]fluoride for labelling tracer molecules it has to be separated from the aqueous phase. One of the first established methods of nucleophilic radiofluorination is the addition of the aminopolyether Kryptofix® 222 (4,7,13,16,21,24-Hexaoxa-1,10-diazabicyclo[8.8.8]-hexacosane) and potassium carbonate to the aqueous solution of [^{18}F]fluoride and consequent thermal evaporation of water as azeotropic mixture with acetonitrile [22].

To facilitate the separation of [^{18}F]fluoride from water the cyclotron-produced aqueous solution is applied on an anion exchange resin to trap the [^{18}F]fluoride and elute it with a mostly organic elution solution containing both an aminopolyether and potassium carbonate [23]. Through this way expensive [^{18}O]H_2O can also be recovered. However, water contents of up to 30 vol-% are still used for the elution and the eluted [^{18}F]fluoride has to be dried by iterative azeotropic evaporation with acetonitrile [24-27]. This is due to the fact that fluoride ions are strongly solvated in protic solvents such as water because of their formation of hydrogen bonds. For a nucleophilic substitution most solvent molecules have to be removed. [28].

Depending on the labelling reaction, columns can be preconditioned in various ways to optimize radiochemical yield and/or avoid decomposition. Most notably, QMA Plus Light columns (Waters; Milford, Massachusetts, USA) come in the quaternary methyl ammonium form and have been diversely conditioned, mostly to convert them either to the bicarbonate [29-32] or carbonate form [25, 33, 34].

Elution solutions can also be prepared with tetraalkylammonium solutions resulting in highly nucleophilic tetraalkylammonium fluoride [35].

An alternative to separate [^{18}F]fluoride from water is the recovery in an electrochemical cell [36].Since its first use by Alexoff et al. [36], this method has been extensively researched [37, 38] and used in several radiosyntheses [39-41]. Electrochemical separation can also be applied to microfluidic systems [42].

Recently, novel methods which directly use the [^{18}F]fluoride eluate for the following radiofluorination without a thermal evaporation step were developed. Approaches include the use of ionic liquids [43] or organic bases instead of inorganic ones [44]. For thermally unstable products, long alkyl chain quaternary ammonium salts can be introduced on a solid phase extraction cartridge allowing quantitative trapping and elution with pure aprotic solvent (acetonitrile, dimethylsulfoxide or dimethylformamide) [45].

As another way to avoid azeotropic drying, potassium hydroxide was used instead of potassium carbonate as source for potassium as central ion in the cryptate complex [46]. This so-called Munich method has already been used for labelling peptides via a silicon-fluoride-acceptor reagent (SiFA), where omitting azeotropic drying resulted in saving 15 to 27 minutes in the preparation of reactive [^{18}F]fluoride [47-50]. In general, avoiding the azeotropic drying step results in a shorter total synthesis time and has many positive implications: less radioactivity is lost due to radioactive decay, a higher reliability is achieved due to a more simple approach, there is less radiation exposure time and fewer exposure risks especially in manual radiosyntheses and also less [^{18}F]fluoride needs to be produced due to fewer radioactivity losses in the setup.

Yet another approach is the reduction of water-content of a conventional elution solution while keeping potassium carbonate and an aminopolyether such as Kryptofix® 222 to form a complex and serve as eluting agent. An elution solution with only four percent water was successfully implemented in the radiosynthesis of 2-[^{18}F]Fluoro-2-deoxy-D-glucose ([^{18}F]FDG). This method still evaporates the eluate to dryness once [51]. Lowering the water portion even more and increasing the concentration of the eluting complex resulted in still viable elution solutions. The complex formation equilibrium is shifted to the cryptate complex by waiting a sufficient amount of time or by adding excess potassium carbonate or Kryptofix® 222, and the potassium cryptate complex is formed even at water contents as low as 1 vol-% [52].

Microfluidic radiosynthesis

Due to the unique properties in a microfluidic system some special advantages arise in comparison to normal vessel-based radiosyntheses. The small radius of the microreactor provides a higher surface to volume ratio. The miniaturization of the reactor also gives a better thermal exchange with the heating device and a more uniform temperature profile thus also making rapid heating or cooling possible. Such an apparatus is also able to withstand higher mechanical strain like pressure [53].

The high pressure that is attainable during microfluidic radiosyntheses raises the boiling point of the solvent thus making it possible to increase the reaction temperature beyond conventionally used temperatures. These higher reaction temperatures usually correspond to a higher incorporation rate with smaller amounts of valuable precursor [27, 54]. Furthermore, the setup allows a facile optimization of reaction parameters and a dose-on-demand production of radiotracers with only one batch of radionuclide solution [55].

The low reaction volume in microreactors also means that a higher concentration of the radionuclide in reaction solution is present if the same amount of radioactive atoms are used compared to vessel-based synthesis. This is especially important considering that the radioactive isotope is only available in subnanomolar concentrations and is therefore in the same concentration range as impurities in solvents and reagents [56].

Additionally, smaller amounts of reagents need to be used in a smaller reactor. This also has implications in the purification steps after the synthesis; the most common being a semi-preparative high performance liquid chromatography (HPLC). A smaller volume of reaction mixture can be purified on a smaller column which is normally more efficient and more reliable due to the better packing of sorbent. Furthermore, a smaller column operates at a lower flow rate which increases the concentration of the product. This comes especially in handy considering that the eluent may be toxic and has to be removed or in case of ethanol has to be below a certain limit [57].

Finally, microfluidic devices are for the most part fully automated systems that can be controlled remotely by computer software. Via this way, high reproducibility and minimal radiation doses for the operator are guaranteed. It has also been suggested that because of the device's geometry, radiolysis in microfluidic radiosyntheses is drastically reduced [58].

On the other hand, there are still disadvantages resulting from the microfluidic setup. For one thing, the radioactivity consists of several milliliters target water and has to be concentrated before being applied in a microreactor setting. Following the reaction it has to be ensured that all of the radiolabelled product is transferred out of the reactor as even the smallest volumes contain highly concentrated radioactive tracer. This is done by sweeping the reactor out with an excess of diluting solvent thus negating the advantages of having to purify only small amounts of volume [59].

Another common problem is the susceptibility to particles in solutions. As the internal diameter of microreactors is very small (Advion NanoTek® reactors: 100 µm), even tiny particles can clog the reactors. Unclogging can be an arduous process which can cause a delay or even a failed synthesis thus reducing the reliability of routine radiosyntheses [60].

Adenosinergic system

Adenosine, a nucleoside ubiquitous in mammalian cells, has many metabolic and structural relations to biologically essential molecules. On the one hand, it is closely related to the nucleotides cyclic adenosine monophosphate (cAMP), adenosine monophosphate (AMP), adenosine diphosphate (ADP) and adenosine triphosphate (ATP). On the other hand it shares structures with coenzymes NAD, FAD and coenzyme A and also with S-Adenosyl-L-methionine (SAM), a methylating agent. Additionally, it has structural equivalents in DNA and RNA [61].

Extracellular adenosine has four categories of effects on cells. It can increase the ratio of oxygen supply to demand, condition cells to protect against ischemic damage, trigger an anti-inflammatory response and it can promote angiogenesis [62].

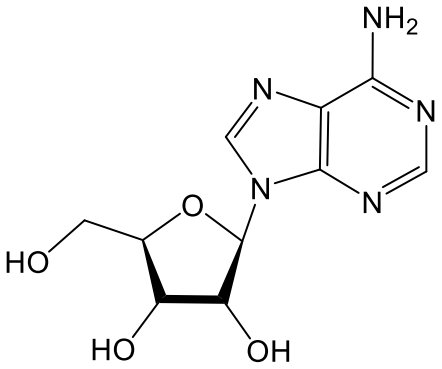

Figure 6: Chemical structure of adenosine

There are currently four known classes of adenosine receptors, namely adenosine A_1, A_{2A}, A_{2B} and A_3 receptors. All of them are G protein-coupled receptors. Their notation stems from the preferred endogenous agonist for all those receptors, adenosine [63].

Amongst others, they are all targeted by caffeine, the most commonly consumed drug in the world, with its effect basing on the interaction with the adenosine receptors. The adenosine A_{2A} receptor is involved in interaction with somnogens like prostaglandin D2 and with caffeine while the adenosine A_1 receptor is shown to be integral to the sleep-wake cycle [64, 65].The receptors are believed to be promising targets in a wide range of conditions, such as arrhythmias, myocardial or cerebral ischemia, pain, neurodegenerative diseases, sleep disorders, inflammation, diabetes, renal failure, cancer and glaucoma [66].

A_1 adenosine receptors are highly expressed in brain, heart, adipose tissue, stomach, vas deferens, testis, spleen, kidney, aorta, liver, eye and bladder. A_{2A} adenosine receptor expression is high in the striatum, nucleus accumbens and olfactory tubercle. At a lower level, it is found in immune cells, heart, lung and blood vessels. A_{2B} receptors are expressed at low levels almost ubiquitously. A_3 receptor

expression has been found in various tissues like spleen, liver, lung, uterus, testis, and bladder and at lower levels in the heart, jejunum, proximal colon, kidney and eye. It was also detected in many brain regions, namely the cortex, amygdala, striatum, olfactory bulb, nucleus accumbens, hippocampus, hypothalamus, thalamus and cerebellum [67].

PET imaging of the A_3 adenosine receptor

FE@SUPPY ([5-(2-fluoroethyl) 2,4-diethyl-3-(ethylsulfanylcarbonyl)-6-phenylpyridine-5-carboxylate)] was first developed by Li et al. [68] in search for a selective A_3 adenosine receptor antagonist among 3,5-diacyl-2,4-dialkylpyridine derivatives. Because of its high affinity to the human A_3 adenosine receptor (K_i = 4.22 nM) and high selectivity (K_i [A_1]/ K_i[A_3] = 2700) demonstrated in this study it was then investigated as the first PET tracer for the A_3 adenosine receptor [69, 70]. Synthesis of [^{18}F]FE@SUPPY was achieved by radiofluorination of the tosylated precursor Tos@SUPPY [5-(2-tosyloxyethyl) 2,4-diethyl-3-(ethylsulfanylcarbonyl)-6-phenylpyridine-5-carboxylate] in acetonitrile. Ester-linked functional groups like the [^{18}F]fluoroethyl label are susceptible to cleaving by carboxylesterases as found in human blood plasma which would result in unspecific binding of radioactive metabolites of [^{18}F]FE@SUPPY if it is applied to the patient [71]. Since Azéma et al. [72] demonstrated an increased stability of thioesters compared to carboxylic esters, radiofluorination on the thioester site rather than on the carboxylic ester site should show a better metabolic profile resulting in the development of [^{18}F]FE@SUPPY:2 [5-ethyl 2,4-diethyl-3-((2-fluoroethyl)sulfanylcarbonyl)-6-phenylpyridine-5-carboxylate][24, 26]. However, metabolite studies refuted those assumptions as FE@SUPPY showed no rat brain metabolites 30 minutes post injection and the blood metabolism was considerably slower [73].

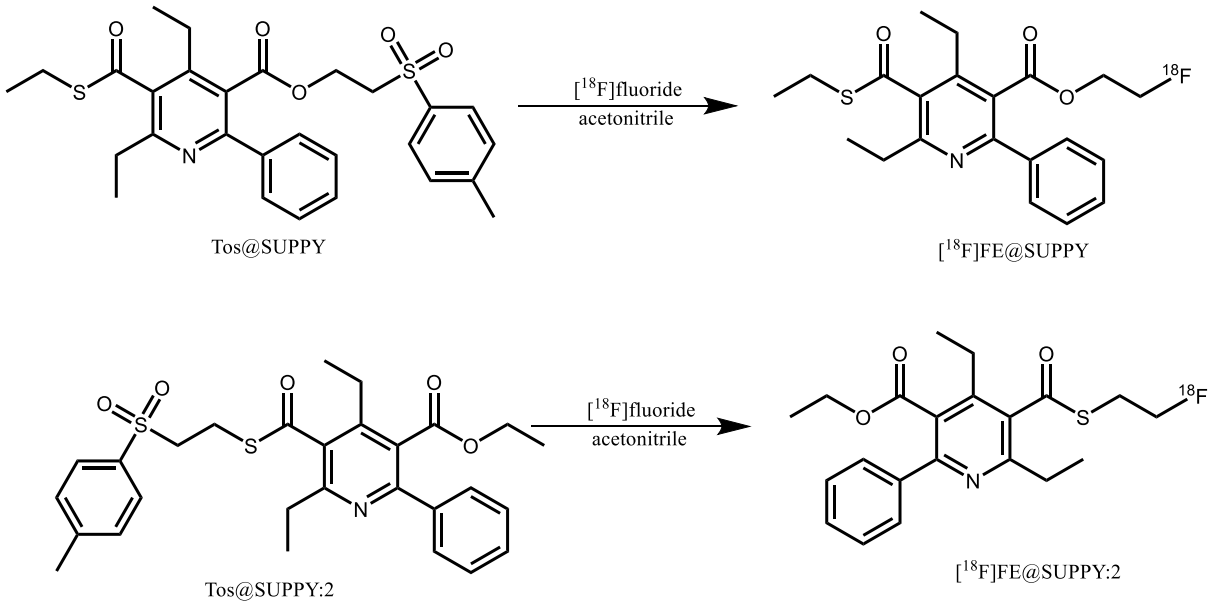

Scheme 5: Reaction mechanism of radiosynthesis of [^{18}F]FE@SUPPY and [^{18}F]FE@SUPPY:2 ([60])

Aim

Fluorine-18 ($t_{1/2}$ = 109.8 min) is one of the most commonly used radionuclides in PET [74]. It provides a perfect compromise between the isotopic labelling with carbon-11 whose half-life ($t_{1/2}$ = 20.4 min) only gives it limited availability and labelling with readily available generator-produced radionuclides like gallium-68 with significant changes in the tracer structure compared to natural ligands [9].

To ensure high specific activity of radiotracers, fluorine-18 is generated in a cyclotron as [^{18}F]fluoride in aqueous solution [17]. As the typical labelling occurs as nucleophilic substitution [^{18}F]fluoride has to be separated from water as the ion is strongly solvated in water and thus unavailable for reactions. Separation and activation usually consists of trapping [^{18}F]fluoride on an anion exchange cartridge, releasing it with an elution solution containing phase-transfer catalysts and drying the eluate azeotropically with acetonitrile [75].

The aim of this thesis was the investigation of novel elution solutions to facilitate the [^{18}F]fluoride activation. The most important factors to consider were that [^{18}F]fluoride is quantitatively released after trapping on a column and that the eluate contained reactive [^{18}F]fluoride for a high incorporation in radiosynthesis. Concurrently, the necessity of azeotropic drying step in different setups was evaluated. Another significant consideration was that these elution solutions could be applied to a microfluidic system where usually more efficient radiosyntheses take place [76].

The elution potency of examined solutions was determined by creating elution profiles considering various commercially available anion exchange cartridges.

The reactivity of the obtained eluate was determined by comparing radiochemical incorporation yields in the exemplary straightforward radiosyntheses of [^{18}F]FE@SUPPY and [^{18}F]FE@SUPPY:2. Radiosyntheses were conducted manually vessel-based and automatically at a microfluidic scale.

Materials and methods

Materials

[^{18}F]Fluoride was produced by irradiation of enriched $H_2{}^{18}O$ (Rotem; Dimona, Israel) via the ^{18}O (p,n) ^{18}F reaction in a GE PETtrace cyclotron (16.5 MeV protons; GE Medical Systems; Uppsala, Sweden). For the following tests residual [^{18}F]fluoride was flushed out of the tubes with 2.5 ml $H_2{}^{16}O$ after production and delivery of high activity [^{18}F]fluoride (15 - 60 GBq) resulting in an aqueous solution with activities of up to 1 GBq.

Solvents

Aqua bidest. "Fresenius" (Fresenius Kabi; Graz, Austria) and acetonitrile for DNA synthesis (Merck; Darmstadt, Austria) were used as solvents for elution solutions, for azeotropic drying and in the reactions. In mobile phases for the TLC and HPLC analysis of product solution, acetonitrile CHROMASOLV® Plus for HPLC ≥ 99.9% (Sigma-Aldrich; Vienna, Austria) and Aqua B. Braun Spüllösung Ecotainer® plus (Braun; Melsungen, Germany) were used.

Elution of [^{18}F]fluoride

For separation of [^{18}F]fluoride from the aqueous phase, it was trapped on different anion exchange cartridges. CHROMAFIX® 30-PS-HCO_3^- solid-phase extraction cartridges (45 mg sorbent) were purchased from Macherey-Nagel (Düren, Germany). ^{18}F Trap & Release Columns (25 mg and 9 mg sorbent) were obtained from ORTG Inc. (Oakdale, Tennessee, USA). Sep-Pak AccelPlus QMA Plus Light cartridges (130 mg sorbent) were purchased from Waters (Milford, Massachusetts, USA). Conventional elution solutions were prepared with Kryptofix® 222 (4,7,13,16,21,24-Hexaoxa-1,10-diazabicyclo[8.8.8]-hexacosane) and potassium carbonate (Merck; Darmstadt, Germany). TBAH * 30 H_2O (tetrabutylammonium hydroxide 30-hydrate), TEAB (tetraethylammonium bicarbonate) and 1 M potassium hydroxide solution (Sigma-Aldrich; Vienna, Austria) were used for other elution solutions.

Radiosynthesis of [^{18}F]FE@SUPPY and [^{18}F]FE@SUPPY:2

Precursors Tos@SUPPY [5-(2-tosyloxyethyl) 2,4-diethyl-3-(ethylsulfanylcarbonyl)-6-phenylpyridine-5-carboxylate] and Tos@SUPPY:2 [5-ethyl 2,4-diethyl-3-((2-tosyloxyethyl)sulfanylcarbonyl)-6-phenylpyridine-5-carboxylate] as well as reference standards FE@SUPPY [5-(2-fluoroethyl) 2,4-diethyl-3-(ethylsulfanylcarbonyl)-6-phenylpyridine-5-carboxylate] and FE@SUPPY:2 [5-ethyl 2,4-diethyl-3-((2-fluoroethyl)sulfanylcarbonyl)-6-phenylpyridine-5-carboxylate] were provided by the Division of Drug Synthesis at the Department of Pharmaceutical Chemistry of the University of Vienna (Austria) [77]. Vessel-based reactions and corresponding azeotropic drying were conducted in 3.0 ml Wheaton v-vials. Reaction vials were sealed with PTFE/Silicone septa (Wheaton; Millville, New Jersey, USA).

For microfluidic radiosyntheses an Advion NanoTek® system (Ithaca, New York, USA) was used. With the suitable Advion software (ver. 1.4.0 GMP Lite) both a concentrator and evaporator module (CE) and a liquid flow reactor (LF) were operated. Reactions were conducted in a microreactor with an inner diameter of 100 µm and a length of 2 m. The fused silica tubing of the reactor was coiled in a brass ring and fixed with thermoresistant tubing. Azeotropic drying was conducted in a 5.0 ml Wheaton v-vial. In these particular syntheses pump 1 was utilized for the precursor solution and pump 3 was used for the [^{18}F]fluoride solution whereas pump 2 remained unused. While acetonitrile for DNA synthesis (Merck; Darmstadt, Germany) was used in the concentrator for azeotropic drying and dissolving the dry [^{18}F]fluoride the other pumps were supplied with acetonitrile CHROMASOLV® Plus for HPLC ≥ 99.9% (Sigma-Aldrich; Vienna, Austria).

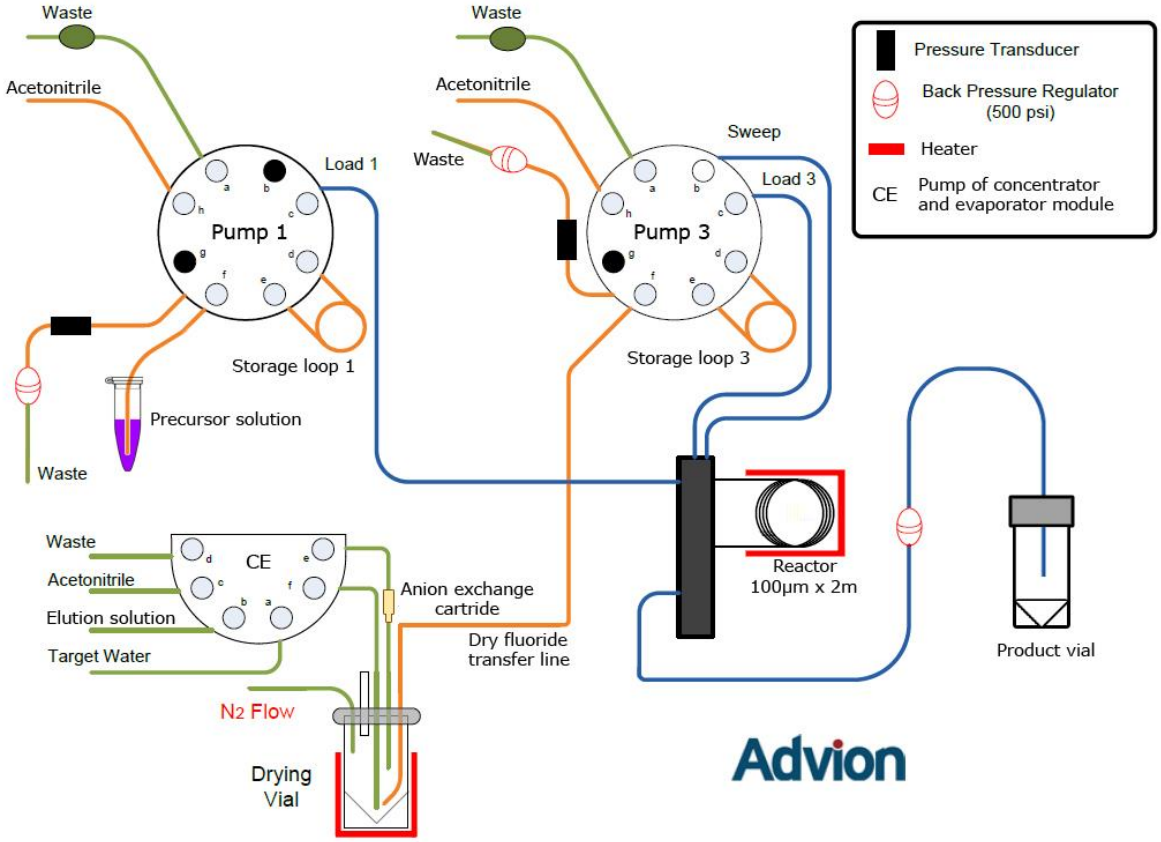

Figure 7: Customized Setup of Advion Nanotek® (Plumbing plan taken from Advion software and modified)

Quality control

Product identity and radiochemical incorporation yield (RCIY) were confirmed via radio-TLC (thin layer chromatography) and radio-HPLC (high performance liquid chromatography) according to Ungersboeck et al. [27]. 1 µl of each product solution was analyzed on TLC Silica gel 60 F_{254} 25 Aluminium sheets (Merck; Darmstadt, Germany) with a 95/5 (v/v) acetonitrile/water mixture as mobile phase. The radio-TLC plates were visualized using an instant imager (Canberra-Packard; Schwadorf, Austria). Radio-HPLC was performed on a system with a Merck-Hitachi LaChrom L-7100 pump, a NaI radiodetector (raytest; Straubenhardt, Germany) and a Merck-Hitachi UV detector (254 nm) on a Merck Chromolith Performance RP-18e 100 x 4.6 mm column using a mixture of acetonitrile, a 2.5 g/l ammonium acetate solution with pH 3.2, and acetic acid [60:38.8:1.2; (v/v/v)] and a flow rate of 2 ml/min. Chromatographic analysis was performed with Gina Star version 5.8 (raytest; Straubenhardt, Germany).

Methods

Preparing of elution solutions

The solution currently in use for eluting [^{18}F]fluoride trapped on an anion exchange cartridge was prepared by dissolving 22 mg Kryptofix® 222 and 4.5 mg potassium carbonate in 1 ml of a 80:20 (v/v) mixture of acetonitrile and water (solution A). Test solutions were prepared by dissolving the same amount of Kryptofix® 222 and potassium carbonate in acetonitrile/water-mixtures with different volume ratios. This resulted in a Kryptofix® 222 concentration of 58.4 µmol/ml and a potassium concentration of 65.1 µmol/ml.

Solution	Acetonitrile content [vol-%]	Water content [vol-%]
A	80	20
B	85	15
C	90	10
D	95	5
E	99	1
F	100	0

Table 2: Composition of different elution solutions with Kryptofix® 222 (22 mg/ml) and potassium carbonate (4.5 mg/ml)

All solutions were freshly prepared for each experiment except for solution E which was incubated over night at 60 °C due to incomplete dissolution. Freshly prepared elution solution E without overnight incubation was indicated as E*. Solution F was prepared by dissolving both Kryptofix® 222 and potassium carbonate in 250 µl water and drying it azeotropically at 100 °C while bubbling through with a constant N_2-stream and while adding acetonitrile iteratively before dissolving the dried residue in pure acetonitrile.

Another elution solution (solution WA) was prepared according to Wester et al. [46] by dissolving 282.4 mg Kryptofix® 222 in 500 µl 1M KOH. This solution was azeotropically dried at 100 °C while bubbling through with a constant N_2-stream and while adding acetonitrile iteratively. The residue was then dissolved in 3 ml acetonitrile, resulting in a Kryptofix® 222 concentration of 250 µmol/ml and a potassium concentration of 167 µmol/ml.

Tetraalkylammonium elution solutions were prepared by dissolving either 15 mg tetraethylammonium bicarbonate (78.4 µmol) or 45 mg tetrabutylammonium hydroxide 30-hydrate (56.3 µmol) in a mixture of 200 µl H_2O and 800 µl acetonitrile.

Elution tests

Elution tests were performed behind lead shielding. Cyclotron-produced [^{18}F]fluoride in $H_2{}^{16}O$ was divided into multiple vials and each one was filled up to 2.5 ml with water resulting in aqueous solutions with activities in the magnitude of 50 - 200 MBq. After the anion exchange column trapped the [^{18}F]fluoride it was purged of residual water with either air and/or acetonitrile. [^{18}F]fluoride was eluted from the column in 100 µl increments of elution solution followed by approximately 200 µl air. Radioactivity of the column was measured after each portion of elution solution and each 100 µl fraction was collected separately and measured. No more than 1 ml of elution solution was used as it would make the following drying procedures more extensive and would also be not advisable for microfluidic syntheses.

Additionally, QMA Plus Light cartridges were conditioned before some elution tests:

	Conditioning
I	10 ml 1M $NaHCO_3$, 10 ml H_2O [29, 30]
II	5 ml 1M potassium carbonate, 15 ml H_2O [25]
III	10 ml 1M potassium carbonate, 20 ml H_2O, 10 ml AcN

Table 3: Conditioning procedures for QMA Plus Light columns

Vessel-based radiosynthesis of [^{18}F]FE@SUPPY and [^{18}F]FE@SUPPY:2

[^{18}F]FE@SUPPY and [^{18}F]FE@SUPPY:2 were prepared at reaction conditions according to Wadsak et al. [69] and Haeusler et al. [24] respectively. Briefly, in a lead-shielded fume hood aqueous [^{18}F]fluoride solution was trapped on an anion exchange column and eluted with 0.7 ml of a previously prepared elution solution (see p.36) into a 3.0 ml Wheaton v-vial. The solvent was evaporated at 100 °C while bubbling through the solution with a nitrogen stream. For azeotropic drying, 0.5 ml acetonitrile were added and the solution was evaporated to dryness again. After drying, a fixed volume of precursor solution in acetonitrile (15 mg/ml Tos@SUPPY or 20 mg/ml Tos@SUPPY:2) was added to the vial. The vial was then sealed tightly and heated at 75 °C for 20 minutes unless otherwise specified. To quench the reaction, twice the volume of water was added to the reaction mixtures and the vials were put on ice. Further purification steps were omitted.

Microfluidic radiosynthesis of [^{18}F]FE@SUPPY:2

Microfluidic reactions were performed according to Ungersboeck et al. [27] in a lead-shielded cell with Advion Nanotek® system. Before each radiosynthesis a preprogrammed macro for cleaning the concentrator element ("Concentrator Clean") and the remaining apparatus ("Master Clean") with acetonitrile were performed. [^{18}F]Fluoride separation from water and consecutive azeotropic drying and dissolving in 500 µl acetonitrile were performed automatically with a macro (see Macros for microfluidic radiosynthesis, p.58). 10 mg/ml Tos@SUPPY:2 solution was freshly prepared and both precursor solution and [^{18}F]fluoride solution were transferred into respective storage loops by utilizing the so-called discovery mode of the software. At first, the tubing from the solution to the storage loop was filled ("Prime") followed by filling of the storage loop ("Fill") and finally loading the tubing from the loop to the microreactor with fluoride or precursor solution ("Load"). Each pump then pushed a defined fraction of the stored solution (50 – 160 µl) into the microreactor with a constant flow rate of 30 µl/min. After each reaction the reactor was swept via pump 3 with 250 µl pure acetonitrile at a flow rate of 60 – 200 µl/min to push out any remaining product from the reactor. The crude product solution was collected in a 1.0 ml Wheaton v-vial and was not purified any further. Quenching the reaction did not have an effect on the yield and was therefore skipped. After each set of syntheses, the preinstalled macro for cleaning the apparatus ("Master Clean") was performed.

The discovery mode is part of the Advion software (ver. 1.4.0 GMP Lite) which enabled the variation of parameters such as temperature, volumes of precursor and isotope solution, pump rate and transfer rate with only one batch of dried fluoride. The setup was operated remotely through the interface as seen in Figure 8. The process of a synthesis was monitored by observing the pressure graphs. As shown in Figure 9, when both pumps pushed precursor or radionuclide solution into the reactor both indicated a constant pressure signal. Then, as the reactor was swept with acetonitrile from pump 3 only that corresponding pressure indicator showed a pressure signal: At first a lower one where the reaction mixture was pushed out of the reactor, then a higher constant pressure where the reactor was flushed out with pure acetonitrile.

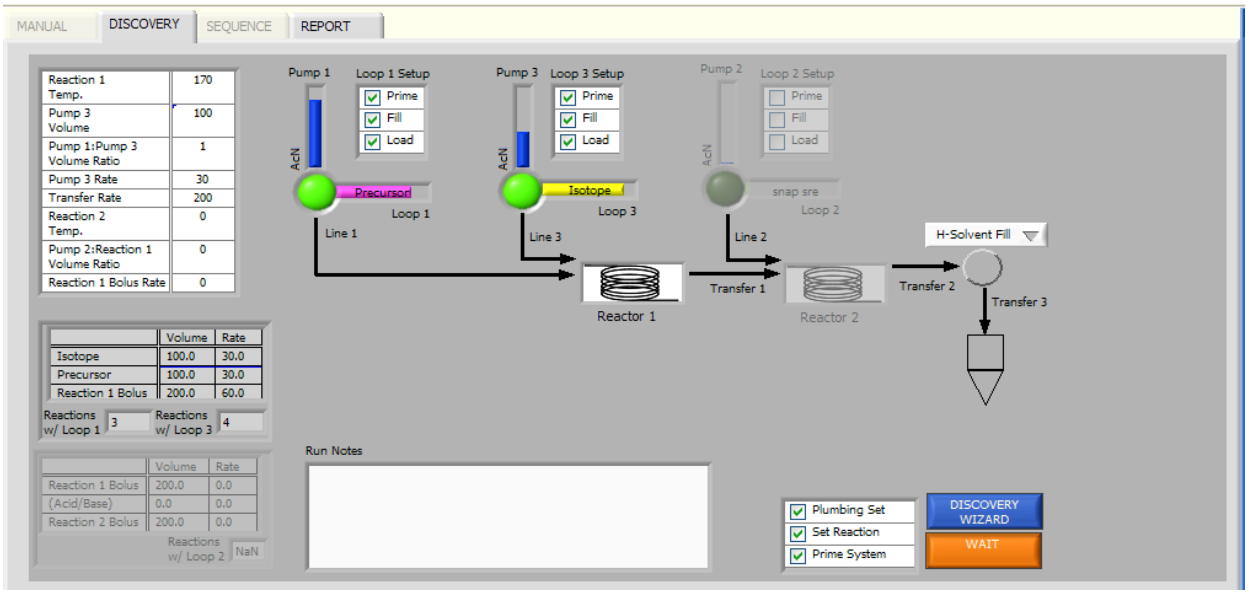

Figure 8: Discovery mode interface of the Advion software (ver. 1.4.0 GMP Lite)

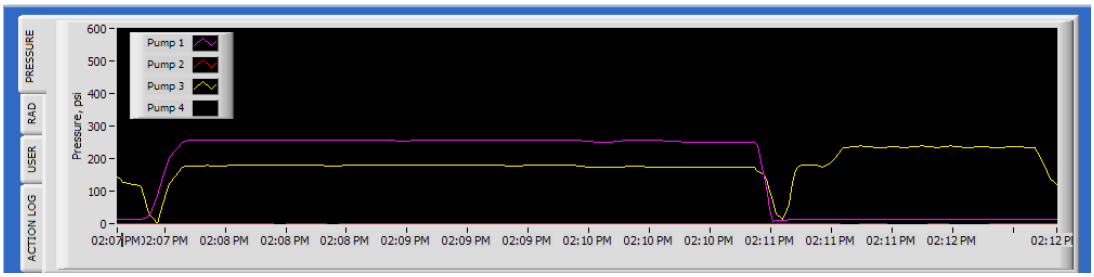

Figure 9: Typical pressure diagram of a microfluidic synthesis

Quality control

For radio-HPLC approx. 30 µl of product solution were injected via a syringe into the HPLC system (20 µl loop) described as above (Quality control, p. 35). Each run lasted 6 minutes. A typical chromatogram (Figure 10) showed distinct peaks for [^{18}F]fluoride and product ([^{18}F]FE@SUPPY or [^{18}F]FE@SUPPY:2). Unlike TLC, parts of [^{18}F]fluoride stayed on the column and remained undetected. Therefore, HPLC merely served as a qualitative analysis method. Precursors Tos@SUPPY and Tos@SUPPY:2 eluted later than the product while other UV absorption peaks stemmed from Kryptofix® 222. No formation of side products or decomposition of product could be detected in the time frame of the analysis.

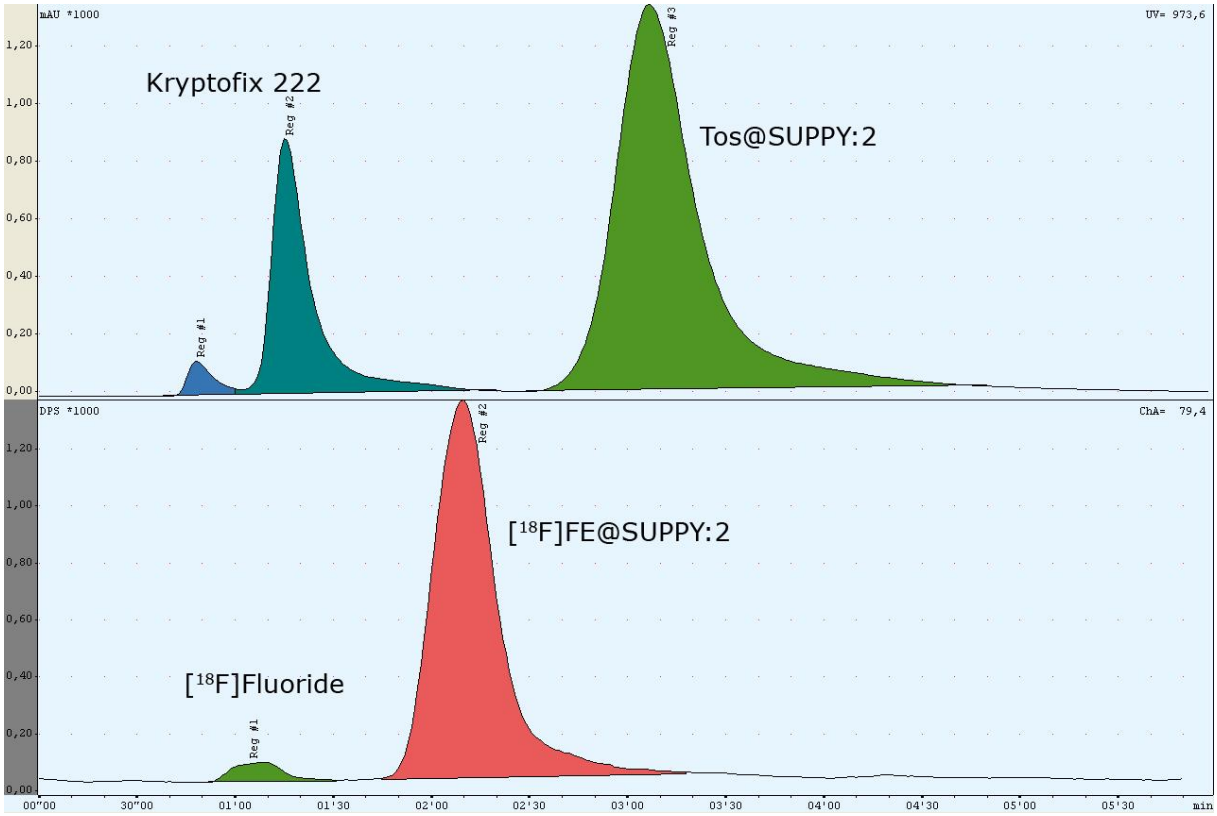

Figure 10: Exemplary chromatogram of [^{18}F]FE@SUPPY:2 crude product from a vessel-based synthesis, eluted with elution solution A . The upper channel shows UV absorption at 254 nm while the lower channel measures the radioactivity.

For radio-TLC, 1 µl of product solution was put on an appropriate TLC plate with a pipette. After it had dried, it was put into the TLC chamber filled with 95/5 (v/v) acetonitrile/water. When the solvent front nearly reached the end of the plate it was taken out and left to dry. Then it was analyzed with an instant imager. [^{18}F]Fluoride stuck to where it was applied on the plate while product was carried by the mobile phase. Thus, the RCIY could be assessed.

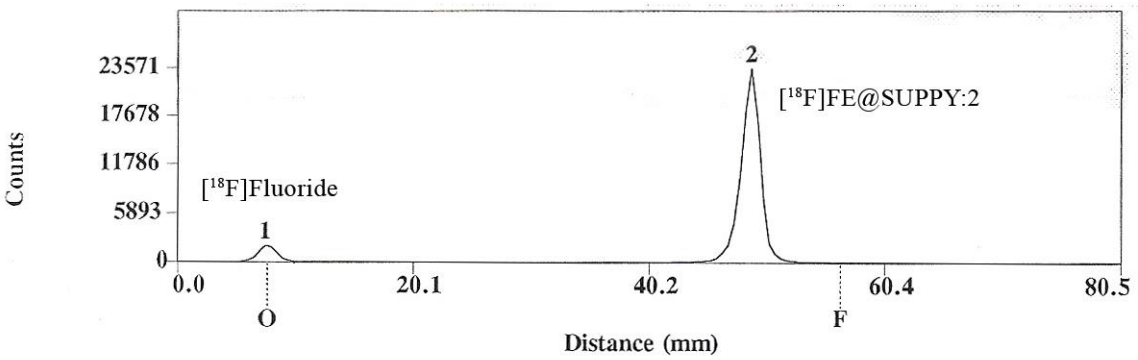

Figure 11: Exemplary thin layer chromatogram of [^{18}F]FE@SUPPY:2 crude product from a microfluidic synthesis, eluted with elution solution A . O denotes the origin where product solution was applied while F indicates the solvent front.

Results

Elution tests

For data comparison, the percentage of [^{18}F]fluoride removed from the anion exchange cartridge was plotted against the volume of elution solution used. Radioactivity measurements in every separate experiment were corrected for decay.

Furthermore, to investigate the removal of 90 % of trapped [^{18}F]fluoride a linear interpolation between the two closest points was used as approximation.

30-PS-HCO_3^- (45 mg)

[^{18}F]Fluoride elution from a 30-PS-HCO_3^- column with 1 ml of routinely used elution solution A occurred with 98.0 ± 1.5 % while at 0.5 ml 78.7 ± 5.5 % was eluted. Only elution solution WA removed slightly more [^{18}F]fluoride from the column, 98.4 ± 0.8 % at 1 ml. Except for solution F which removed 32.7 ± 9.7 % all elution solutions removed over 90 % of trapped [^{18}F]fluoride at 1 ml.

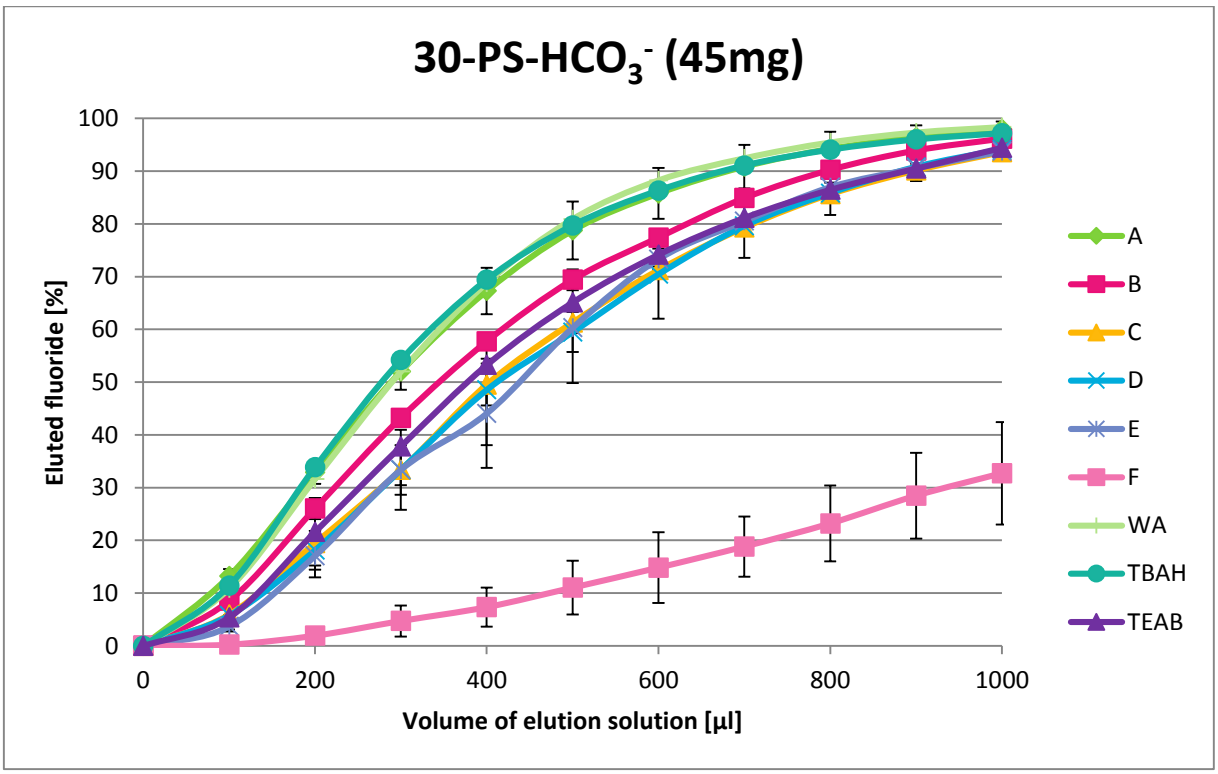

Figure 12: [^{18}F]Fluoride elution profiles of different elution solutions with a 30-PS-HCO_3^- cartridge (45 mg sorbent)

	% Fluoride removed from column			90% removed at [µl]
	with 0.5 ml	with 1 ml	n	
A	78.7 ± 5.5	98.0 ± 1.5	2	683.0 ± 28.9
B	69.4 ± 2.0	96.2 ± 1.1	2	795.7 ± 5.7
C	61.3 ± 2.0	93.6 ± 0.7	2	897.1 ± 8.4
D	59.5 ± 9.6	94.1 ± 1.9	2	883.7 ± 26.0
E	60.3 ± 4.6	93.7 ± 0.0	2	883.7 ± 7.7
F	11.0 ± 5.1	32.7 ± 9.7	2	-
WA	80.9 ± 4.6	98.4 ± 0.8	2	641.5 ± 20.3
TBAH	79.7 ± 1.3	97.2 ± 0.6	2	677.6 ± 6.3
TEAB	65.1 ± 12.3	94.4 ± 3.8	2	887.2 ± 55.0

Table 4: Data of [^{18}F]fluoride elution on a 30-PS-HCO_3^- cartridge (45 mg sorbent)

QMA Plus Light (130 mg)

98.9 ± 0.5 % of [^{18}F]fluoride trapped on QMA Plus Light cartridges was removed by 1 ml of elution solution A and 50.2 ± 24.8 % by 0.5 ml. Solution E only removed 6.9 ± 2.9 % while solution F did not elute any radioisotope from the column.

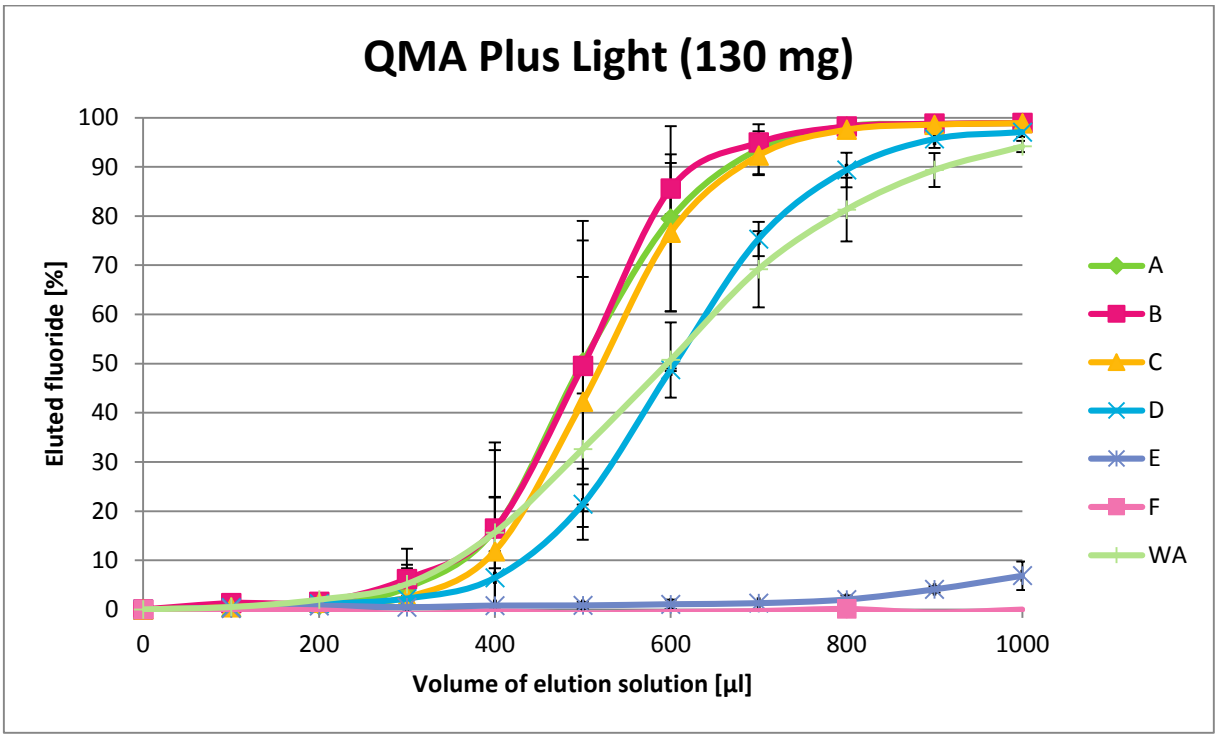

Figure 13: [^{18}F]Fluoride elution profiles of different elution solutions with a QMA Plus Light cartridge (130 mg sorbent)

	% Fluoride removed from column			90% removed at [µl]
	with 0.5 ml	with 1 ml	n	
A	50.2 ± 24.8	98.9 ± 0.5	2	674.6 ± 57.7
B	49.5 ± 29.5	98.9 ± 0.4	2	647.1 ± 24.9
C	42.2 ± 25.4	98.9 ± 0.4	2	685.5 ± 38.9
D	21.4 ± 7.2	97.1 ± 1.0	2	810.2 ± 27.2
E	0.8 ± 0.7	6.9 ± 2.9	2	-
F	-0.4 ± 0.5	0.0 ± 1.3	2	-
WA	32.6 ± 11.3	94,1 ± 1.2	2	913.5 ± 28.8
TBAH	31.4 ± 5.7	99,1 ± 0.2	2	738.9 ± 54.2
TEAB	11.3 ± 1.2	87,1 ± 5.0	2	-

Table 5: Data of [^{18}F]fluoride elution on a QMA Plus Light cartridge (130 mg sorbent)

Fluoride Trap & Release Column (25 mg)

[^{18}F]Fluoride was released from the Fluoride Trap & Release (25 mg sorbent) column completely with 1 ml of the conventional elution solution A while 0.5 ml elution solution removed 99.7 ± 0.1 %. Solutions B through E also eluted more than 90 % even with 0.5 ml eluent volume.

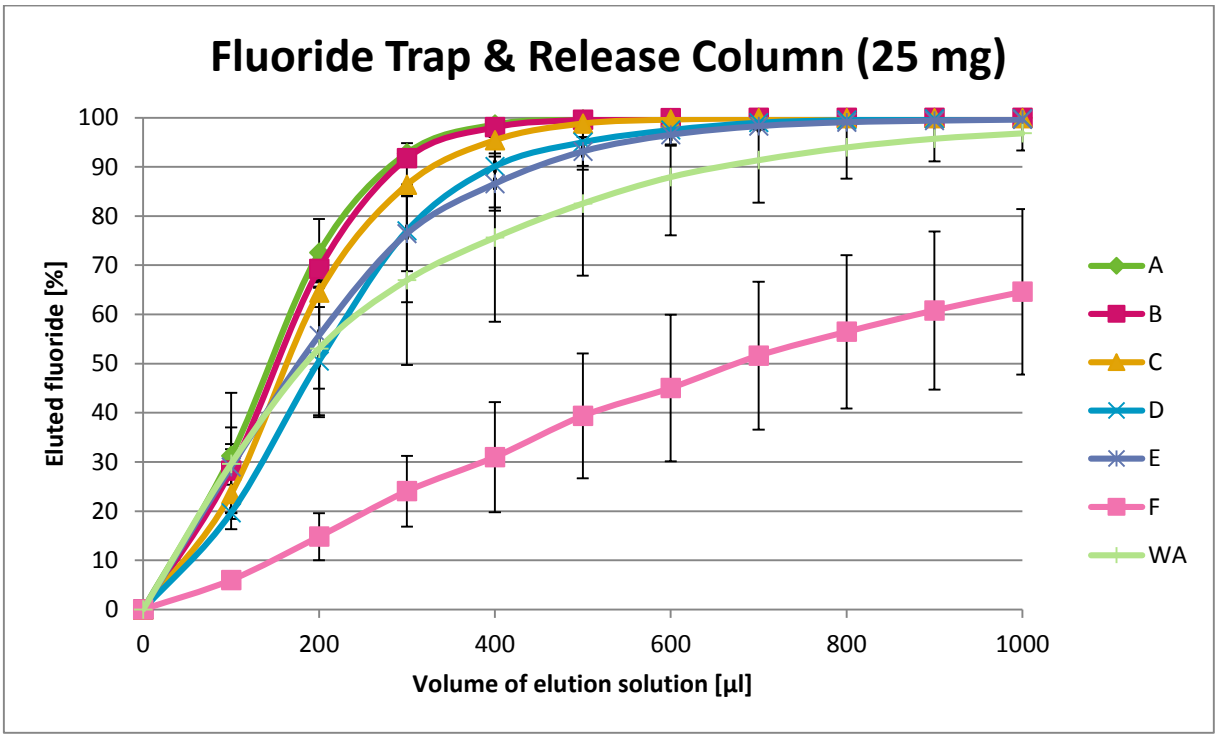

Figure 14: [^{18}F]Fluoride elution profiles of different elution solutions with a Fluoride Trap & Release column (25 mg sorbent)

	% Fluoride removed from column			90% removed at [µl]
	with 0.5 ml	with 1 ml	n	
A	99.7 ± 0.1	100.0 ± 0.0	2	286.3 ± 7.9
B	99.6 ± 0.0	100.0 ± 0.0	2	292.3 ± 1.1
C	98.8 ± 0.5	99.9 ± 0.0	2	340.2 ± 1.0
D	95.0 ± 5.6	99.8 ± 0.3	2	399.3 ± 33.4
E	93.1 ± 2.9	99.6 ± 0.2	2	452.1 ± 18.8
F	39.4 ± 12.7	64.6 ± 16.8	2	-
WA	82.5 ± 14.7	96.8 ± 3.5	2	660.4 ± 65.5

Table 6: Data of [^{18}F]fluoride elution on a Fluoride Trap & Release cartridge (25 mg sorbent)

Fluoride Trap & Release Column (9 mg)

On Fluoride Trap & Release (9 mg sorbent) columns elution solution A removed 99.0 ± 1.1 % at 0.5 ml and 99.9 ± 0.0 % at 1 ml volume of eluent. While solutions B, D, E and E* nearly completely removed [^{18}F]fluoride with 1 ml elution solution 1 ml of solution F removed 80.1 ± 9.6 %.

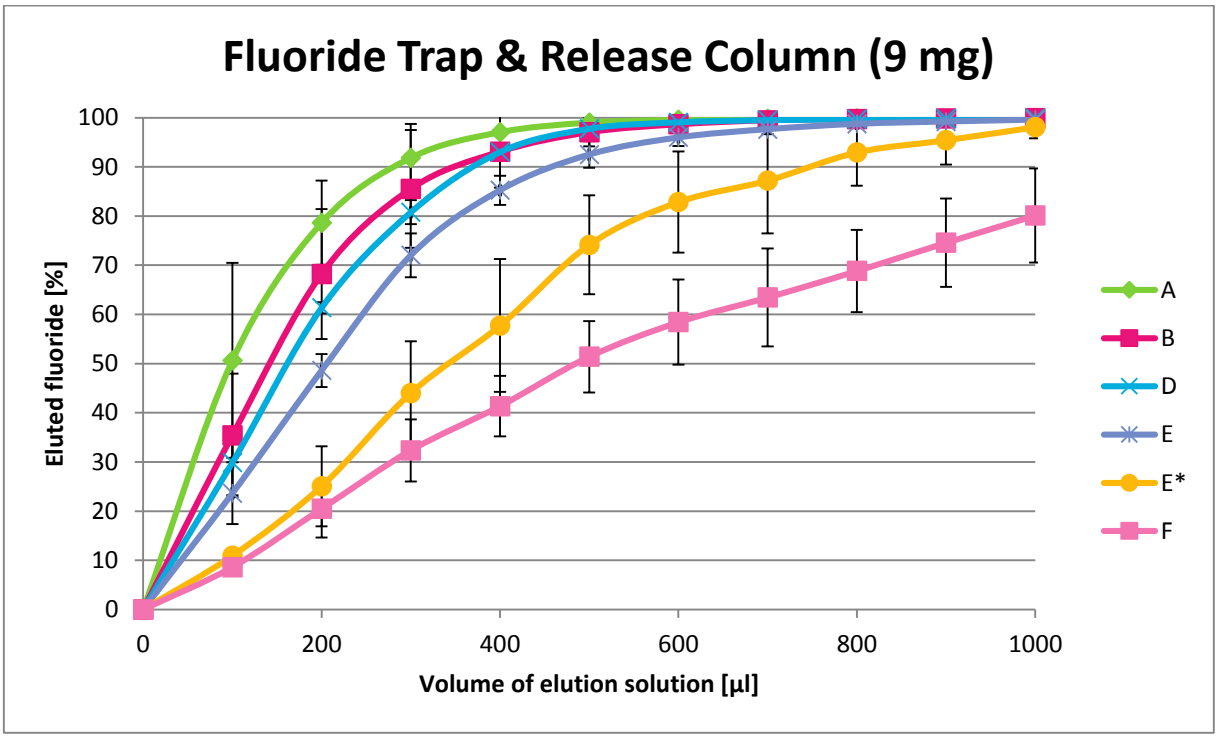

Figure 15: [^{18}F]Fluoride elution profiles of different elution solutions with a Fluoride Trap & Release column (9 mg sorbent)

	% Fluoride removed from column			90% removed at [µl]
	with 0.5 ml	with 1 ml	n	
A	99.0 ± 1.1	99.9 ± 0.0	2	285.9 ± 20.3
B	97.0 ± 2.9	99.9 ± 0.1	2	359.2 ± 33.2
D	97.8 ± 0.3	99.9 ± 0.0	2	375.3 ± 6.2
E	92.5 ± 2.7	99.6 ± 0.0	2	465.6 ± 12.9
E*	74.2 ± 10.1	98.1 ± 2.3	2	748.6 ± 66.1
F	51.4 ± 7.3	80.1 ± 9.6	2	-

Table 7: Data of [^{18}F]fluoride elution on a Fluoride Trap & Release cartridge (9 mg sorbent)

Column comparison

Elution solution A released [^{18}F]fluoride almost completely from all columns. 1 ml solution A removed 98.0 ± 1.5 % from 30-PS-HCO_3^-, 98,9 ± 0.5 % from QMA Plus Light, 100.0 ± 0.0 % from Fluoride Trap & Release (25 mg) and 99.9 ± 0.0 % from Fluoride Trap & Release (9 mg) cartridges.

A more notable difference could be detected at 0.5 ml elution solution used: 78.7 ± 5.5 % was released from 30-PS-HCO_3^-, 50.2 ± 24.8 % from QMA Plus Light, 99.7 ± 0.1 % from Fluoride Trap & Release (25 mg) and 99.0 ± 1.1 % from Fluoride Trap & Release (9 mg).

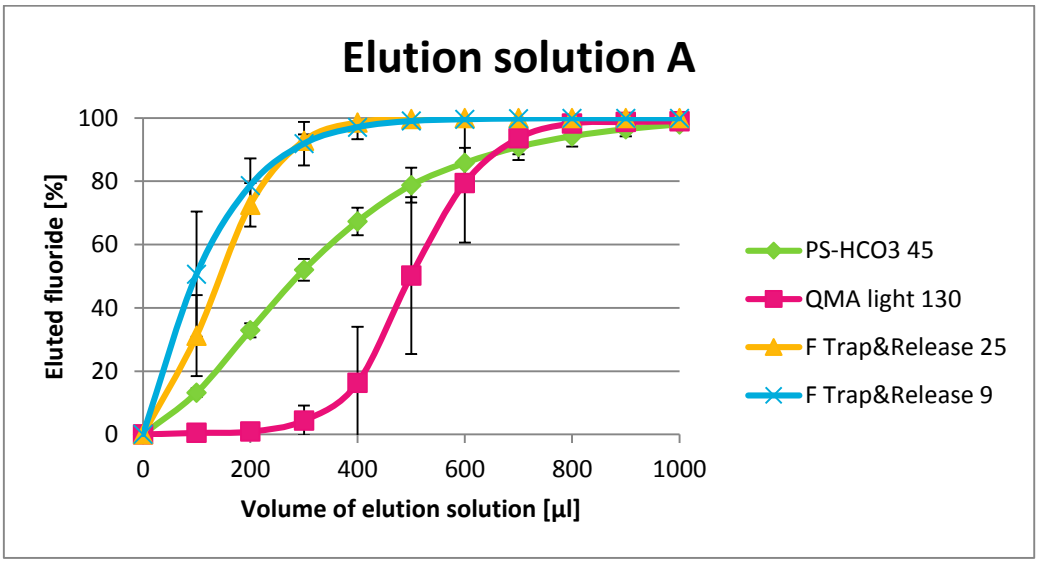

Figure 16: [^{18}F]Fluoride elution profiles of elution solution A on different anion exchange cartridges

Column	% Fluoride removed from column			90% removed at [µl]
	with 0.5 ml	with 1 ml	n	
30-PS-HCO_3^- (45 mg)	78.7 ± 5.5	98.0 ± 1.5	2	683.0 ± 28.9
QMAPlus Light (130 mg)	50.2 ± 24.8	98,9 ± 0.5	2	674.6 ± 57.7
Fluoride Trap & Release (25 mg)	99.7 ± 0.1	100.0 ± 0.0	2	286.3 ± 7.9
Fluoride Trap & Release (9 mg)	99.0 ± 1.1	99.9 ± 0.0	2	285.9 ± 20.3

Figure 17: Data of [^{18}F]fluoride elution on different columns with elution solution A

Comparison of conditioning procedures

1 ml of elution solution A released 98.9 ± 0.5 % of trapped [^{18}F]fluoride from an unconditioned QMA Plus Light column. If columns were conditioned with 10 ml 1M $NaHCO_3$ and 10 ml H_2O (conditioning I), 99.3 ± 0.2 % were eluted. Conditioning II (5 ml 1M potassium carbonate and 15 ml H_2O) resulted in 99.8 ± 0.1 % release while conditioning III (10 ml 1M potassium carbonate, 20 ml H_2O and 10 ml AcN) resulted in 98.7 ± 1.4 % release with 1 ml of elution solution.

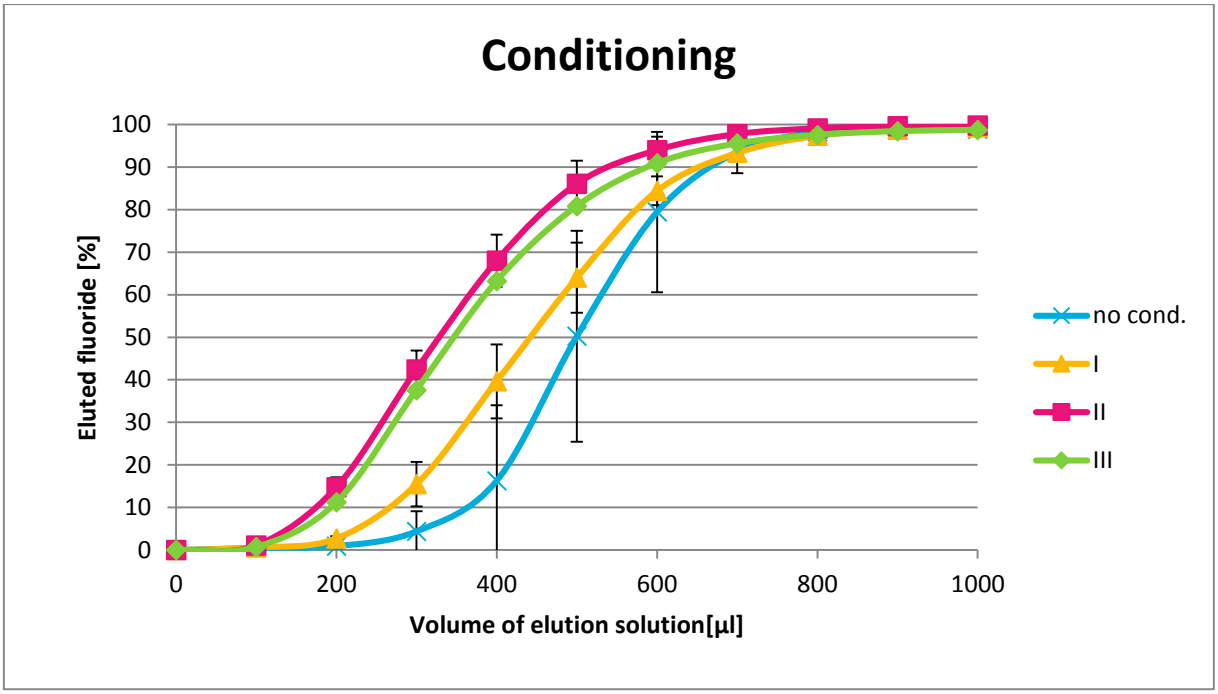

Figure 18: [^{18}F]Fluoride elution profiles of elution solution A on QMA Plus Light columns (130 mg sorbent) with different conditioning procedures

Conditioning	% Fluoride removed from column			90% removed at [µl]
	with 0.5 ml	with 1 ml	n	
no	50.2 ± 24.8	98.9 ± 0.5	2	674.6 ± 57.7
I	64.0 ± 8.3	99.3 ± 0.2	2	662.5 ± 14.5
II	86.1 ± 5.5	99.8 ± 0.1	2	549.7 ± 23.7
III	80.8 ± 0.4	98.7 ± 1.4	2	590.9 ± 7.8

Table 8: Data of [^{18}F]fluoride elution with solution A on QMA Plus Light columns (130 mg sorbent) with different conditioning procedures

Vessel-based radiosynthesis of [^{18}F]FE@SUPPY and [^{18}F]FE@SUPPY:2

[^{18}F]FE@SUPPY

At first, [^{18}F]FE@SUPPY radiosyntheses were performed at 100 °C after elution from a Fluoride Trap & Release column (25 mg) with a reaction volume of 125 µl. 14.7 % radiochemical incorporation yield (RCIY) was achieved with azeotropically dried [^{18}F]fluoride eluted via the routinely used elution solution A. Reactions with solution WA eluted [^{18}F]fluoride resulted in a RCIY of 2.5 ± 0.8 % and 1.3 ± 1.4 %, with and without azeotropic drying respectively. Elution with solution E resulted in 19.6 ± 3.7 % (azeotropically dried) and 16.7 ± 8.3 % (not azeotropically dried) incorporation.

For 30-PS-HCO_3^- cartridges at a reaction volume of 125 µl and at 75 °C, standard conditions (elution solution A, azeotropically dried eluate) resulted in 13.4 % incorporation. Without azeotropic drying, 3.4 % of [^{18}F]fluoride was incorporated. Reaction mixtures diluted with 125 µl acetonitrile showed generally lower yields: 8.2 % and 7.1 % for [^{18}F]fluoride eluted with solution E and azeotropically dried and not azeotropically dried, respectively and 11.4 % azeotropically dried solution A eluate.

Elution solution	Azeotropically dried?	RCIY [%]	n
E	yes	19.6 ± 3.7	2
E	no	16.7 ± 8.3	2
WA	yes	2.5 ± 0.8	3
WA	no	1.3 ± 1.4	3
A	yes	14.7	1

Table 9: Radiochemical incorporation yields (RCIYs) of [^{18}F]fluoride into [^{18}F]FE@SUPPY after elution on a Fluoride Trap & Release column (25 mg) at a reaction temperature was 100 °C

Elution solution	Azeotropically dried?	Other	RCIY [%]	n
E	yes	Reaction mixture diluted with 125 µl acetonitrile	8.2	1
E	no		7.1	1
A	yes		11.4	1
A	yes		13.9	1
A	no		3.4	1

Table 10: Radiochemical incorporation yields (RCIYs) of [^{18}F]fluoride into [^{18}F]FE@SUPPY after elution on a 30-PS-HCO_3^- anion exchange cartridge (45 mg sorbent)

[^{18}F]FE@SUPPY:2

With a reaction volume of 250 µl the following radiochemical incorporation yields (RCIYs) were achieved after eluting [^{18}F]fluoride from a PS-HCO_3^-. Relative RCIY was calculated by dividing the RCIY by the RCIY of routinely used conditions (azeotropically dried [^{18}F]fluoride eluted with elution solution A).

Elution solution	Azeotropically dried?	RCIY [%]	Relative RCIY [%]	n
A	No	0.5 ± 0.2	3.1 ± 1.3	5
A	Yes	15.7 ± 13.5	100.0 ± 86.1	9
A	Yes (x2)	18.1 ± 8.9	115.2 ± 57.0	2
A	Yes (x3)	25.5 ± 18.8	162.8 ± 119.7	2
C	Yes	28.9 ± 27.9	184.0 ± 178.1	2
D	No	12.4 ± 13.6	78.7 ± 87.0	2
D	Yes	25.0 ± 3.6	159.2 ± 23.1	4
E	No	8.5 ± 1.6	54.2 ± 9.9	2
E	Yes	9.8 ± 2.0	62.5 ± 12.8	3
WA	No	1.2 ± 1.0	7.7 ± 6.2	4
WA	Yes	1.2 ± 0.9	7.7 ± 5.9	4

Table 11: Radiochemical incorporation yields (RCIYs) of [^{18}F]fluoride into [^{18}F]FE@SUPPY:2 after elution on a PS-HCO_3^- anion exchange cartridge (45 mg sorbent). 250 µl precursor solution was used for reactions.

The following RCIYs were achieved with 500 µl reaction volume after trapping and eluting [^{18}F]fluoride on a PS-HCO_3^- anion exchange cartridge:

Elution solution	Azeotropically dried?	RCIY [%]	Relative RCIY [%]	n
A	Yes	34.7 ± 3.0	100.0 ± 8.7	10
C	Yes	23.6 ± 11.6	68.0 ± 33.4	2
D	No	34.9 ± 28.8	100.6 ± 83.0	3
D	Yes	31.7 ± 2.0	91.2 ± 5.8	2
E	No	21.6 ± 6.3	62.1 ± 18.1	2
E	Yes	31.6 ± 5.2	91.0 ± 15.1	2
TEAB	No	8.8 ± 8.6	25.2 ± 24.6	2
TEAB	Yes	11.7 ± 1.6	33.5 ± 4.7	2
TBAH	No	46.1 ± 2.3	132.8 ± 6.5	2
TBAH	Yes	21.0 ± 3.9	60.6 ± 11.1	3

Table 12: Radiochemical incorporation yields (RCIYs) of [^{18}F]fluoride into [^{18}F]FE@SUPPY:2 after elution on a PS-HCO_3^- anion exchange cartridge (45 mg sorbent). 500 µl precursor solution was used for reactions.

Microfluidic radiosynthesis of [^{18}F]FE@SUPPY:2

All reaction solutions were pumped into the microreactor with a speed of 30 µl/min. Unless otherwise noted, PS-HCO_3^- anion exchange columns (45 mg sorbent) were used. Same volumes of precursor solution and [^{18}F]fluoride solution were used in each reaction. The following radiochemical incorporation yields were achieved:

Eluted with	Azeotropic drying?[a]	Temperature [°C]	Precursor solution volume [µl]	Transfer rate [µl/min]	RCIY [%]	n
A	Yes	160	59-100	60-200	82.2 ± 23.4	9
A	Yes	170	59-100	200	88.1 ± 6.3	2
A	Yes[c]	160	59-100	200	17.2 ± 6.1	4
A	Yes[c]	170	59-100	200	23.5 ± 9.2	4
D	Yes	160	59-159	60-200	72.4 ± 7.7	9
E	No[d]	160	159	120-200	6.0 ± 0.1	2
E	No[e]	160	59-100	60-120	0.7 ± 0.3	4
E	No	150	65-106	200	17.7 ± 9.9	3
E	No	160	59-106	120-200	40.6 ± 24.5	6
E	No	170	65-106	200	29.1 ± 12.6	3
TBAH/3[b]	Yes	160	59-100	200	18.1 ± 10.4	4
TBAH/3[b]	Yes	170	59-100	200	17.1 ± 10.4	4
TBAH	No	160	81-119	200	0.6 ±0.6	6
TBAH	Yes	160	100-119	200	97.5 ± 1.2	6
TEAB	Yes	160	59-100	200	18.5 ± 5.9	2
TEAB	Yes	170	59-100	200	19.5 ± 1.6	2

Table 13: Radiochemical incorporation yields (RCIYs) of [^{18}F]fluoride into [^{18}F]FE@SUPPY:2 after elution on a PS-HCO_3^- anion exchange cartridge (45 mg sorbent). Precursor and [^{18}F]fluoride solution were pumped into the microreactor at 30 µl/min. Same volumes of both solutions were used.

[a] Azeotropic drying was performed with macro #1 (Table 14,p. 58) while elution without azeotropic drying was performed with macro #2 (Table 16, p. 60)

[b] For TBAH/3 solution, only 15 mg instead of 45 mg TBAH*30 H_2O were used.

[c] QMA Plus Light (130 mg sorbent) was used for fluoride trapping.

[d] [^{18}F]fluoride was trapped and eluted manually and directly pumped into the microfluidic system.

[e] The azeotropic drying macro was stopped after elution with 1 ml elution solution.

Discussion

Elution tests

Elution tests with the conventional elution solution A served successfully as a proof of concept of the set up with all four columns used in the study [PS-HCO_3^-, QMA Plus Light and Fluoride Trap & Release (25 or 9 mg)].

For elution solutions with different ratios of water but same eluting agents (B-E), only a slight decrease in ability to elute [^{18}F]fluoride was observable. A notable decrease of elution ability was evidenced only on QMA Plus Light columns.

Overnight incubation at 60 °C as part of preparation of elution solution E is beneficial as demonstrated in elution tests on Fluoride Trap & Release (9 mg) columns. If freshly prepared, over one and a half times of eluent volume is required to remove 90 % of trapped [^{18}F]fluoride.

Anhydrous elution solution F proved to be limited in its ability to elute [^{18}F]fluoride. As quantitative removal was not achieved on any column, investigations about the reactivity of the eluate were omitted.

Even though 1 ml of solution A is sufficient to remove almost all [^{18}F]fluoride in all tested columns, there is clear trend that a higher sorbent amount corresponds to later elution of the radionuclide. While both Fluoride Trap & Release columns released at least 99 % with 0.5 ml of elution solution A the same amount only removed 50.2 ± 24.8 % from QMA Plus Light columns.

Solution WA with potassium hydroxide instead of potassium carbonate proved to be a feasible alternative for elution of [^{18}F]fluoride as it showed comparable ability to release trapped [^{18}F]fluoride from PS-HCO_3^- cartridges. On other columns elution was slightly less effective if compared to standard solutions. The noteworthy advantage is that the eluate contains no water and can swiftly be evaporated if required. Possibly, use of another cartridge (QMA Carbonate Plus Light, 46 mg sorbent) can optimize [^{18}F]fluoride release as in literature [48-50]. In the same protocols [48-50], the dried potassium cryptate was freshly dissolved in anhydrous acetonitrile for each experiment stating that the solution should be expended in 5 to 10 minutes while in this thesis a batch of WA solution was prepared and used in more than one experiment in the course of some days. This may be the cause for more unsuccessful results than expected.

Conditioning of QMA Plus Light columns indicated a slightly earlier release of [^{18}F]fluoride. Conditioning methods with potassium carbonate solution (II and III) showed an increased capability of releasing [^{18}F]fluoride with smaller volumes of elution solution.

Vessel-based radiosynthesis of [^{18}F]FE@SUPPY and [^{18}F]FE@SUPPY:2

Ungersboeck et al. [27] reported a RCIY of 88.2 ± 3.4 % at 75 °C for 20 min with 15 mg/ml precursor for [^{18}F]FE@SUPPY and 42.5 ± 7.2 % for [^{18}F]FE@SUPPY:2 with 20 mg/ml precursor.

[^{18}F]FE@SUPPY incorporation could not be replicated in such a manner. A possible reason for that is that in literature [^{18}F]FE@SUPPY was prepared automatically in a GE TRACERlab fx unit, while in this thesis it was prepared manually in a lead-shielded fume hood. Another notable change was the lower volume of the reaction. One 500 µl solution of Tos@SUPPY (15 mg/ml) was split into four parts to vary more parameters within one experiment. After azeotropic drying, fluoride can adsorb to the wall of the v-vials and is potentially not properly resolubilized in these small amounts of acetonitrile [78]. Furthermore, high reaction temperatures in the range of the boiling point of acetonitrile (81.6 °C) may have caused irreproducible conditions. The use of a different column did not cause any incorporation deficiencies.

Another deviation from conventional radiosyntheses in literature, both vessel-based and microfluidic, is the [^{18}F]fluoride solution. Normally, [^{18}F]fluoride is obtained by directly transferring irradiated [^{18}O]H_2O into a suitable vial for the synthesis. In this thesis, as only small amounts of radioactivity were needed, so that [^{18}F]fluoride from a previous radionuclide production that had remained in the transfer line was pushed out with regular deionized water.

Experiments for [^{18}F]FE@SUPPY syntheses could not be repeated entirely because no more precursor was available.

For [^{18}F]FE@SUPPY:2, reactions with 250 µl precursor solution still yielded significant unreliability and less than satisfactory incorporation yields. Thus, 500 µl precursor solution was used for later reactions. The magnitude of incorporation yield, 34.7 ± 3.0 % (elution solution A, azeotropically dried eluate), is comparable to that in literature (42.5 ± 7.2 % [27]), especially considering that different set ups were used for the synthesis. Azeotropic drying of eluates of solutions with lower water content (C, D, E) did not improve incorporation of [^{18}F]fluoride.

Despite being an elution solution free from water and thus alluding to a higher reactivity of [^{18}F]fluoride, solution WA was not investigated at 500 µl reaction volume as the incorporation at 250 µl was particularly low, barely exceeding 1 %. In successful labelling reactions with similar solutions in literature, QMA Plus Light columns were preconditioned and used for elution [46] or oxalic acid was added to the reaction mixture while different columns were used [48-50]. Furthermore, slightly different amounts of substances were used for preparing the elution solution: 0.5 ml were prepared with 100 µl 1 M KOH and 41 mg Kryptofix® 222.

Elution with TBAH showed a considerable improvement of incorporation yield, 46.1 ± 2.3 %, even without azeotropic drying. It should be noted that contrary to other reactions azeotropic drying considerably reduced the incorporation yield to 21.0 ± 3.9 %. This could support the notion that [^{18}F]fluoride may be adsorbed to the walls of the reaction vials during the drying process and thus impairing the reactivity.

Microfluidic radiosynthesis of [^{18}F]FE@SUPPY:2

Previous radiosyntheses of [^{18}F]FE@SUPPY:2 showed a radiochemical incorporation yield of 95.5 ± 1.9 % [27]. The set up could be replicated with elution solution A resulting in a RCIY of 82.2 ± 23.4 %. Quenching the raw product solution with water did not have any significant effect on yield or product stability in the timeframe of the analysis and was therefore omitted. Generally, noteworthy standard deviations were observed. These may stem from the hygroscopic nature of the anhydrous acetonitrile in the pump reservoirs as the solvent was not exchanged before each synthesis [79]. Incorporation yield seems to be dependent on the type of column as the reaction after eluting [^{18}F]fluoride with solution A from a QMA Plus Light column resulted only in an incorporation yield of 17.2 ± 6.1 %.

Radiochemical incorporation yield was unaffected by the volume of reaction as variation from 59 µl to 159 µl did not show any significant aberrations.

Unlike presumptions that lower initial water content in elution solutions results in a lower water content in the dried [^{18}F]fluoride and thus a higher reactivity [28] azeotropic drying after elution of [^{18}F]fluoride with solution D with lower water content resulted in a lower incorporation than with the conventional conditions, 72.4 ± 7.7 %.

Primarily, time could be saved by increasing the transfer speed after each synthesis from the established method from 60 µl/min to 200 µl/min. The radiochemical incorporation yield remained unaffected by this change. This resulted in reduction of synthesis time by 3 minutes.

Elution with TBAH solution followed by azeotropic drying resulted in a particularly high incorporation yield, 97.5 ± 1.2 % (160 °C). Applying the short [^{18}F]fluoride drying macro without the azeotropic drying step (Table 16; p. 60) resulted in surprisingly low conversion of 0.6 ± 0.6 %. It should be noted that at lower concentrations (TBAH/3) only 18.1 ± 10.4 % was incorporated.

The highest [^{18}F]fluoride incorporation yield with the macro omitting the azeotropic drying step (Table 16; p. 60) was achieved by elution with solution E, 40.6 ± 24.5 %. Integration of the short macro resulted in 5 minutes time reduction.

Incorporation yield was not affected by temperature changes from 160 to 170 °C. Only at 150 °C there was a more noticable drop in yield.

Adversities and optimizations of the microfluidic system

Although there are many advantages of a microfluidic synthesis in comparison with a conventional vessel-based synthesis there are still some problems to be worked out in the Advion Nanotek® system, the most common issue being blockage of microreactors due to the small inner diameter [56, 60]. When the microreactor is blocked the pressure of the system increases up to 400 psi (27.6 bar) at which point the pumps automatically halt. To unclog the reactor pure acetonitrile can be pushed through to remove the congestion after releasing the pressure and reversing the reactor. If the reactor is still blocked the pump 3 solvent reservoir can be changed from pure acetonitrile to a 50:50 (v/v) mixture of acetonitrile/water or even 30:70 (v/v) dimethyl sulfoxide/water. Thereby particles that would not be soluble in acetonitrile may be dissolved. After unclogging, the reactor has to be flushed with acetonitrile to remove remains of other solvents.

An alternative to avoid clogging the microreactor is the use of elution solutions containing phase-transfer catalysts like tetrabutylammonium hydroxide or tetraethylammonium bicarbonate instead of the usual combination of Kryptofix® 222 and potassium carbonate as they appeared to be better soluble, even in pure acetonitrile.

For synthesis optimization the already established macro for drying [^{18}F]fluoride (Table 14; p.58) was modified. Briefly, the routinely used macro traps [^{18}F]fluoride on the column, recovers the water and elutes [^{18}F]fluoride with 1 ml elution solution. It is dried azeotropically under a nitrogen stream at 110 °C and by adding two portions of 500 µl acetonitrile (DNA synthesis grade). After cooling down, the dried [^{18}F]fluoride is dissolved in 500 µl of the solvent from pump 3, in this case acetonitrile. This macro can therefore also be used for labelling reactions that take place in other solvents such as dimethyl sulfoxide.

The first new macro (Table 15; p. 59) changes only the last step of the established macro by dissolving the dried [^{18}F]fluoride in 500 µl DNA synthesis grade acetonitrile from the concentrator pump instead of the solvent from pump 3, thus ensuring a lower water content and a higher reactivity consequently.

The second new macro (Table 16; p. 60) shortens the time consumed by azeotropic drying significantly by 5 minutes. After the same trapping and elution steps as in the established method, no acetonitrile is added and the elution solution is dried at 110 °C under a constant nitrogen stream and dissolved in 500 µl solvent from pump 3. This macro is to be used for elution solutions with already low water content or solutions containing very reactive phase-transfer catalysts ensuring sufficient radiochemical yield at minimal elapsed time for radiosynthesis.

Conclusion and outlook

This thesis investigated the facilitation of [^{18}F]fluoride separation from water and a resulting activation for nucleophilic substitutions. For this purpose, novel elution solutions for releasing [^{18}F]fluoride from an anion exchange cartridge were examined. The first attempt was the incremental reduction of water content in elution solutions from 20 % to 0 % while keeping the conventionally used amount of potassium carbonate and Kryptofix® 222. Further examined elution solutions adopted potassium hydroxide as potassium source for the potassium Kryptofix® 222 complex in a water-free solution while a third type utilized tetraalkylammonium salts to elute and activate [^{18}F]fluoride with the conventional amount of water.

In the conventional elution solution reducing the water content to 1 % showed a comparable albeit slightly worse elution potency. Water-free elution solution with potassium hydroxide also showed an elution ability in the same magnitude. Both tetraalkylammonium salts also readily eluted [^{18}F]fluoride in an equal measure.

Even though with 1 ml of elution solution all tested columns readily removed a bulk of trapped [^{18}F]fluoride, columns with a lower sorbent amount released major portions with a lower amount of elution solution.

The reactivity of [^{18}F]fluoride was evaluated by performing a modified radiosynthesis of established radiotracers [^{18}F]FE@SUPPY and [^{18}F]FE@SUPPY:2. Radiosynthesis was performed manually in a lead-shielded fume hood and automatically at a microfluidic scale with an Advion NanoTek® system.

Radiochemical incorporation yields in manual vessel-based radiosynthesis could not be reproduced from literature and showed a considerable standard deviation between repeats. Elution solutions with lower water content resulted in higher yields if azeotropically dried. Water-free potassium hydroxide and Kryptofix® 222 solution showed next to no conversion of [^{18}F]fluoride even when drying the eluate azeotropically.

Microfluidic automated synthesis produced comparable yields to the established method. Other potassium carbonate and Kryptofix® 222 solutions diminished the incorporation efficiency and even with lowered water content, azeotropic drying proved to be crucial. Tetrabutylammonium hydroxide solution improved the incorporation yield slightly compared to conventional methods. Overall, radiosynthesis could be shortened by increasing the reactor sweeping velocity from 60 µl/min to 200 µl/min without sacrificing yield. The 3 minute time saving is especially beneficial if more than one batch is synthesized consecutively. A newly developed macro to omit any addition of acetonitrile for drying while reducing the time significantly did not find any applications yet.

TBAH elution solution proved to be most suitable for [^{18}F]FE@SUPPY:2 radiosyntheses. The [^{18}F]fluoride elution potency equals that of conventionally used elution solution. Even without azeotropic drying, 32.8 % more [^{18}F]fluoride is incorporated during the vessel-based synthesis. In the microfluidic setup, a 10.7 % increase was observed albeit with the azeotropic drying step.

For the future, potassium carbonate and Kryptofix® 222 solutions with reduced water content could be tested on other established [^{18}F]fluorination reactions to establish a more general sense of feasibility. Potassium hydroxide cryptate elution solutions may have to be adjusted in their concentration to find a balance between elution efficiency and reactivity of [^{18}F]fluoride. Tetraalkylammonium salts may prove to be advantageous in other established syntheses especially in a microfluidic setup, where potassium carbonate and Kryptofix® 222 solutions tend to cause clogging problems.

Appendix

Macros for microfluidic radiosynthesis

Time delay [ms]	Command	Action
0	/3o8V4000A48000R	P3 : fill syringe
0	L3702000100004D-L3602000300004E-	Heat concentrator 1 up to 100° C
1000	/5go1V3200A12000M2000o5V1200A0M500G 3go6V6400A12000M1000o1A0G4R	CE: Load Target Water
120000	/7U2M5000U1M5000u2R	G: Turn on Nitrogen
10000	/5o2V1000P12000o5V1000D12000R	CE: add 1 ml elution solution
60000	/5o3V2000A6000M2000o5V75D4800o6V75D 1200o2V2000A0R	CE: Add 0.5 mL acetonitrile
10000	L3702000110004E-L3602000300004E-	Heat concentrator 1 up to 110° C
200000	/5o3V200P6000o5gv650D1M24G6000R	CE: Add 0.5 mL acetonitrile
200000	L37020000260054-L3602000300004E-	CE: Set Heater to 26 °C
150000	/7u1R	G: Turn off Nitrogen
1000	/3o6V10000D24000R	P3: solve Activity in 500 µL solvent

Table 14: Macro for [^{18}F]fluoride trapping and elution, followed by azeotropic drying (already established)

Time delay [ms]	Command	Action
0	/3o8V4000A48000R	P3 : fill syringe
0	L3702000100004D-L3602000300004E-	Heat concentrator 1 up to 100 °C
1000	/5go1V3200A12000M2000o5V1200A0M500G3go6V6400A12000M1000o1A0G4R	CE: Load Target Water
120000	/7U2M5000U1M5000u2R	G: Turn on Nitrogen
10000	/5o2V1000P12000o5V1000D12000R	CE: add 1 ml elution solution
60000	/5o3V2000A6000M2000o5V75D4800o6V75D1200o2V2000A0R	CE: Add 0.5 mL acetonitrile
10000	L3702000110004E-L3602000300004E-	Heat concentrator 1 up to 110 °C
200000	/a5o3V200P6000o5gv650D1M24G6000R	CE: Add 0.5 mL acetonitrile
200000	L37020000260054-L3602000300004E-	CE: Set Heater to 26 °C
150000	/7u1R	G: Turn off Nitrogen
1000	/5o3V400P6000o5gv1000D1M24G6000R	CE: solve Activity in 500 µl acetonitrile

Table 15: Macro for [^{18}F]fluoride trapping and elution, followed by azeotropic drying (dissolving fluoride in acetonitrile)

Time delay [ms]	Command	Action
0	/3o8V4000A48000R	P3 : fill syringe
0	L3702000110004E-L3602000300004E-	Heat concentrator 1 up to 110 °C
1000	/5go1V3200A12000M2000o5V1200A0M500 G3go6V6400A12000M1000o1A0G4R	CE: Load Target Water
85000	/7U2M5000U1M5000u2R	G: Turn on Nitrogen
5000	/5o2V1000P12000o5V1000D12000R	CE: add 1 ml elution solution
210000	L37020000260054-L3602000300004E-	CE: Set Heater to 26 °C
150000	/7u1R	G: Turn off Nitrogen
1000	/3o6V10000D24000R	P3: solve Activity in 500 µL solvent

Table 16: Macro for [^{18}F]fluoride trapping and elution, without azeotropic drying

Abbreviations

A_1, A_{2A}, A_{2B}, A_3	Subtypes of the adenosine receptor
AcN	Acetonitrile
ADP	Adenosine diphosphate
AMP	Adenosine monophosphate
ATP	Adenosine triphosphate
Bq	Becquerel
cAMP	Cyclic adenosine monophosphate
DMSO	Dimethyl sulfoxide
DNA	Deoxyribonucleic acid
EC	Electron capture
FAD	Flavin adenine dinucleotide
FE@SUPPY	5-(2-fluoroethyl) 2,4-diethyl-3-(ethylsulfanylcarbonyl)-6-phenylpyridine-5-carboxylate
FE@SUPPY:2	5-ethyl 2,4-diethyl-3-((2-fluoroethyl)sulfanylcarbonyl)-6-phenylpyridine-5-carboxylate
GMP	Good manufacturing practice
H_2O	Water
HPLC	High performance liquid chromatography
K_i	Inhibitory constant (conventional unit: nM)
Kryptofix® 222	4,7,13,16,21,24-Hexaoxa-1,10-diazabicyclo[8.8.8]-hexacosane
NAD	Nicotinamide adenine dinucleotide
$NaHCO_3$	Sodium bicarbonate
NaI	Sodium iodide
PET	Positron emission tomography
PS-HCO_3^-	Polystyrene bicarbonate
psi	Pound-force per square inch
QMA	Quaternary methyl ammonium
RCIY	Radiochemical incorporation yield

RNA	Ribonucleic acid
SAM	S-Adenosyl-L-methionine
SPECT	Single photon emission computed tomography
TBAH	Tetrabutylammonium hydroxide
TEAB	Tetraethylammonium bicarbonate
$t_{1/2}$	Half-life
TLC	Thin layer chromatography
Tos@SUPPY	5-(2-tosyloxyethyl) 2,4-diethyl-3-(ethylsulfanylcarbonyl)-6-phenylpyridine-5-carboxylate
Tos@SUPPY:2	5-ethyl 2,4-diethyl-3-((2-tosyloxyethyl)sulfanylcarbonyl)-6-phenylpyridine-5-carboxylate

Curriculum Vitae

Personal Details

Name	Maximilian Emberger
Date of birth	October 7th, 1990
Place of birth	Munich, Germany
Nationality	Austria

Education

1996 – 2000	Primary school at Volksschule Bad Häring
2000 – 2008	Secondary school at Bundesrealgymnasium Wörgl
2008	High school diploma (“Matura”) passed with distinction
2008 – 2012	Bachelor study of Chemistry at University of Innsbruck
09/2012	Degree: Bachelor of Science
	Bachelor’s thesis: „Cloning and DNA sequencing of quail CDT1 promoter segments” at the Institute of Biochemistry, Innsbruck (Advisor: Ao.Univ.-Prof. Markus Hartl)
since 2012	Master’s study in Chemistry at the University of Vienna
2014 – 2015	Master’s thesis: „Optimization of [^{18}F]fluoride activation for microfluidic radiosynthesis“ at the Division of Nuclear Medicine, Vienna (Advisor: Assoc. Prof. Dr. Wolfgang Wadsak)

Professional Experience

2009 - 2013	Summer internship at Sandoz Kundl (Quality assurance)

Languages

German	native
English	fluent

References

1. J.-V. Kratz and K.H. Lieser, *Nuclear and Radiochemistry: Fundamentals and Applications*. 2013, 933.
2. G. Choppin, J.-O. Liljenzin, J. Rydberg, and C. Ekberg, *Unstable Nuclei and Radioactive Decay*, in *Radiochemistry and Nuclear Chemistry*, G.C.-O.L.R. Ekberg, Editor. 2013, p. 85-123.
3. M.F. L'Annunziata, *Radiation Physics and Radionuclide Decay*, in *Handbook of Radioactivity Analysis*, M.F. L'Annunziata, Editor. 2012, p. 1-162.
4. S.R. Cherry, J.A. Sorenson, and M.E. Phelps, *Positron Emission Tomography*, in *Physics in Nuclear Medicine*, S.R. Cherry, Editor. 2012, p. 307-343.
5. J.T. Bushberg, J.A. Seibert, E.M.J. Leidholdt, and J.M. Boone, *The Essential Physics of Medical Imaging*. 2 ed. 2002.
6. K.H. Lieser, *Nuclear and Radiochemistry: Fundamentals and Applications*. 2 ed. 2001.
7. M.F. L'Annunziata, *Radioactivity: Introduction and History: Introduction and History*. 2007, 634.
8. I. Velikyan, *Radionuclides for Imaging and Therapy in Oncology*, in *Cancer Theranostics*, X. Chen and S. Wong, Editors. 2014, p. 285-325.
9. W. Wadsak and M. Mitterhauser, *Basics and principles of radiopharmaceuticals for PET/CT.* European Journal of Radiology, 2010. **73**(3): p. 461-469.
10. G.B. Saha, *Basics of PET Imaging: Physics, Chemistry, and Regulations*. 2010.
11. P.W. Miller, N.J. Long, R. Vilar, and A.D. Gee, *Synthesis of ^{11}C, ^{18}F, ^{15}O, and ^{13}N Radiolabels for Positron Emission Tomography.* Angewandte Chemie International Edition, 2008. **47**(47): p. 8998-9033.
12. G.B. Saha, *Fundamentals of Nuclear Pharmacy*. 2 ed. 1992.
13. G. Choppin, J.-O. Liljenzin, J. Rydberg, and C. Ekberg, *Particle Accelerators*, in *Radiochemistry and Nuclear Chemistry*, G.C.-O.L.R. Ekberg, Editor. 2013, p. 493-512.
14. S.R. Cherry, J.A. Sorenson, and M.E. Phelps, *Decay of Radioactivity*, in *Physics in Nuclear Medicine*, S.R. Cherry, Editor. 2012, p. 31-42.
15. S.R. Cherry, J.A. Sorenson, and M.E. Phelps, *Radionuclide and Radiopharmaceutical Production*, in *Physics in Nuclear Medicine*, S.R. Cherry, Editor. 2012, p. 43-61.
16. R.J. Kowalsky and S.W. Falen, *Radiopharmaceuticals in Nuclear Pharmacy and Nuclear Medicine*. 2nd ed. 2004.
17. E. Hess, G. Blessing, H.H. Coenen, and S.M. Qaim, *Improved target system for production of high purity [18F]fluorine via the 18O(p,n)18F reaction.* Applied Radiation and Isotopes, 2000. **52**(6): p. 1431-1440.
18. G. Visser, C. Bakker, J. Herscheid, G. Brinkman, et al., *The chemical properties of [^{18}F]-acetylhypofluorite in acetic acid solution.* J Label Compd Radiopharm, 1984. **21**: p. 1226.
19. R. Chirakal, G. Firnau, G. Schrobilgenn, J. McKay, et al., *The synthesis of [^{18}F]xenon difluoride from [^{18}F]fluorine gas.* Appl Radiat Isot, 1984. **35**: p. 401-404.
20. P.A. Schubiger, L. Lehmann, and M. Friebe, *PET Chemistry: The Driving Force in Molecular Imaging*. 2007.
21. J. Ruth T and P. Wolf A, *Absolute Cross Sections for the Production of ^{18}F via the ^{18}O(p, n)^{18}F Reaction*, in *Radiochimica Acta*. 1979, p. 21.
22. K. Hamacher, H.H. Coenen, and G. Stöcklin, *Efficient Stereospecific Synthesis of No-Carrier-Added 2-[^{18}F]-Fluoro-2-Deoxy-D-Glucose Using Aminopolyether Supported Nucleophilic Substitution.* Journal of Nuclear Medicine, 1986. **27**(2): p. 235-238.
23. D.M. Jewett, S.A. Toorongian, M.A. Bachelor, and M.R. Kilbourn, *Extraction of [^{18}F]fluoride from [^{18}O]water by a fast fibrous anion exchange resin.* Int J Rad Appl Instrum A, 1990. **41**(6): p. 583-6.
24. D. Haeusler, M. Mitterhauser, L.-K. Mien, K. Shanab, et al., *Radiosynthesis of a novel potential adenosine A3 receptor ligand, 5-ethyl-2,4-diethyl-3-((2-[^{18}F]fluoroethyl)sulfanylcarbonyl)-6-phenylpyridine-5-carboxylate ([^{18}F]FE@SUPPY:2).* Radiochimica Acta, 2009. **97**(12): p. 753-758.

25. K. Hayashi, K. Furutsuka, M. Takei, M. Muto, et al., *High-yield automated synthesis of [^{18}F]fluoroazomycin arabinoside ([^{18}F]FAZA) for hypoxia-specific tumor imaging.* Applied Radiation and Isotopes, 2011. **69**(7): p. 1007-1013.
26. M. Mitterhauser, D. Haeusler, L.-K. Mien, J. Ungersboeck, et al., *Automatisation and First Evaluation of [^{18}F]FE@SUPPY:2, an Alternative PET-Tracer for the Adenosine A_3 Receptor: A Comparison with [^{18}F]FE@SUPPY.* The Open Nuclear Medicine Journal, 2009. **1**: p. 15-23.
27. J. Ungersboeck, C. Philippe, L.-K. Mien, D. Haeusler, et al., *Microfluidic preparation of [^{18}F]FE@SUPPY and [^{18}F]FE@SUPPY:2 — comparison with conventional radiosyntheses.* Nuclear Medicine and Biology, 2011. **38**(3): p. 427-434.
28. R.J. Ouellette and J.D. Rawn, *Nucleophilic Substitution and Elimination Reactions*, in *Organic Chemistry*, R.J. Ouellette and J.D. Rawn, Editors. 2014, p. 333-356.
29. L. Wang, B.P. Lieberman, K. Ploessl, and H.F. Kung, *Synthesis and evaluation of ^{18}F labeled FET prodrugs for tumor imaging.* Nucl Med Biol, 2014. **41**(1): p. 58-67.
30. L. Wang, Z. Zha, W. Qu, H. Qiao, et al., *Synthesis and evaluation of ^{18}F labeled alanine derivatives as potential tumor imaging agents.* Nuclear Medicine and Biology, 2012. **39**(7): p. 933-943.
31. M.E. Rodnick, B.G. Hockley, P. Sherman, C. Quesada, et al., *Novel fluorine-18 PET radiotracers based on flumazenil for $GABA_A$ imaging in the brain.* Nucl Med Biol, 2013. **40**(7): p. 901-5.
32. J.W. Seo, B.S. Lee, S.J. Lee, S.J. Oh, et al., *Fast and Easy Drying Method for the Preparation of Activated [^{18}F]Fluoride Using Polymer Cartridge.* Bull. Korean Chem. Soc, 2011. **32**(1): p. 71-76.
33. E. von Guggenberg, J.A. Sader, J.S. Wilson, S. Shahhosseini, et al., *Automated synthesis of an ^{18}F-labelled pyridine-based alkylating agent for high yield oligonucleotide conjugation.* Applied Radiation and Isotopes, 2009. **67**(9): p. 1670-1675.
34. O. Fedorova, O. Kuznetsova, M. Stepanova, V. Maleev, et al., *A facile direct nucleophilic synthesis of O-(2-[^{18}F]fluoroethyl)-L-tyrosine ([^{18}F]FET) without HPLC purification.* J Radioanal Nucl Chem, 2014(301): p. 505-512.
35. D.P. Cox, J. Terpinski, and W. Lawrynowicz, *"Anhydrous" tetrabutylammonium fluoride: a mild but highly efficient source of nucleophilic fluoride ion.* The Journal of Organic Chemistry, 1984. **49**(17): p. 3216-3219.
36. D. Alexoff, D.J. Schlyer, and A.P. Wolf, *Recovery of [^{18}F]fluoride from [^{18}O]water in an electrochemical cell.* International Journal of Radiation Applications and Instrumentation. Part A. Applied Radiation and Isotopes, 1989. **40**(1): p. 1-6.
37. K. Hamacher, T. Hirschfelder, and H.H. Coenen, *Electrochemical cell for separation of [^{18}F]fluoride from irradiated ^{18}O-water and subsequent no carrier added nucleophilic fluorination.* Applied Radiation and Isotopes, 2002. **56**(3): p. 519-523.
38. F. Kügler, D. Roehrens, M. Stumpf, C. Drerup, et al., *Optimizing the transfer of [^{18}F]fluoride from aqueous to organic solvents by electrodeposition using carbon electrodes.* Applied Radiation and Isotopes, 2014. **91**(0): p. 1-7.
39. K. Hamacher and H.H. Coenen, *No-carrier-added nucleophilic ^{18}F-labelling in an electrochemical cell exemplified by the routine production of [^{18}F]altanserin.* Applied Radiation and Isotopes, 2006. **64**(9): p. 989-994.
40. A. Helfer, J. Castillo Meleán, J. Ermert, A. Infantino, et al., *Bis(4-benzyloxyphenyl)iodonium salts as effective precursors for the no-carrier-added radiosynthesis of 4-[^{18}F]fluorophenol.* Applied Radiation and Isotopes, 2013. **82**(0): p. 264-267.
41. S. Sadeghi, V. Liang, S. Cheung, S. Woo, et al., *Reusable electrochemical cell for rapid separation of [^{18}F]fluoride from [^{18}O]water for flow-through synthesis of ^{18}F-labeled tracers.* Applied Radiation and Isotopes, 2013. **75**(0): p. 85-94.
42. R. Wong, R. Iwata, H. Saiki, S. Furumoto, et al., *Reactivity of electrochemically concentrated anhydrous [^{18}F]fluoride for microfluidic radiosynthesis of ^{18}F-labeled compounds.* Applied Radiation and Isotopes, 2012. **70**(1): p. 193-199.
43. H.W. Kim, J.M. Jeong, Y.-S. Lee, D.Y. Chi, et al., *Rapid synthesis of [^{18}F]FDG without an evaporation step using an ionic liquid.* Applied Radiation and Isotopes, 2004. **61**(6): p. 1241-1246.

44. C.F. Lemaire, J.J. Aerts, S. Voccia, L.C. Libert, et al., *Fast Production of Highly Reactive No-Carrier-Added [^{18}F]Fluoride for the Labeling of Radiopharmaceuticals.* Angewandte Chemie International Edition, 2010. **49**(18): p. 3161-3164.
45. J. Aerts, S. Voccia, C. Lemaire, F. Giacomelli, et al., *Fast production of highly concentrated reactive [^{18}F] fluoride for aliphatic and aromatic nucleophilic radiolabelling.* Tetrahedron Letters, 2010. **51**(1): p. 64-66.
46. H.J.P. Wester, G. Henriksen, and S.H. Weßmann, *Method for the direct elution of reactive [^{18}F]fluoride from an anion exchange resin in an organic medium suitable for radiolabelling without any evaporation step by the use of alkalimetal and alkaline earth metal cryptates*, W.I.P. Organization,WO 2011/141410 A1, 2011
47. R. Koudih, A. Kostikov, M. Kovacevic, D. Jolly, et al., *Automated radiosynthesis of N-succinimidyl 3-(di-tert-butyl[^{18}F]fluorosilyl)benzoate ([^{18}F]SiFB) for peptides and proteins radiolabeling for positron emission tomography.* Applied Radiation and Isotopes, 2014. **89**(0): p. 146-150.
48. B. Wängler, A.P. Kostikov, S. Niedermoser, J. Chin, et al., *Protein labeling with the labeling precursor [^{18}F]SiFA-SH for positron emission tomography.* Nat. Protocols, 2012. **7**(11): p. 1964-1969.
49. C. Wängler, S. Niedermoser, J. Chin, K. Orchowski, et al., *One-step ^{18}F-labeling of peptides for positron emission tomography imaging using the SiFA methodology.* Nat. Protocols, 2012. **7**(11): p. 1946-1955.
50. A.P. Kostikov, J. Chin, K. Orchowski, E. Schirrmacher, et al., *Synthesis of [^{18}F]SiFB: a prosthetic group for direct protein radiolabeling for application in positron emission tomography.* Nat. Protocols, 2012. **7**(11): p. 1956-1963.
51. N.A. Gomzina, D.A. Vasil'ev, and R.N. Krasikova, *Optimization of Automated Synthesis of 2-[^{18}F]Fluoro-2-deoxy-D-glucose Involving Base Hydrolysis.* Radiochemistry, 2002. **44**(4): p. 403-409.
52. D. Eshima, M. Husnu, H. Padgett, T.A. Klausing, et al., *Methods and compositions for drying in the preparation of radiopharmaceuticals*. 2013.
53. P.W. Miller, A.J. deMello, and A.D. Gee, *Application of Microfluidics to the Ultra-Rapid Preparation of Fluorine-18 Labelled Compounds.* Current Radiopharmaceuticals, 2010. **3**(3): p. 254-262.
54. V. Bouvet, M. Wuest, P.-H. Tam, M. Wang, et al., *Microfluidic technology: An economical and versatile approach for the synthesis of O-(2-[^{18}F]fluoroethyl)-l-tyrosine ([^{18}F]FET).* Bioorganic & Medicinal Chemistry Letters, 2012. **22**(6): p. 2291-2295.
55. G. Pascali, G. Mazzone, G. Saccomanni, C. Manera, et al., *Microfluidic approach for fast labeling optimization and dose-on-demand implementation.* Nuclear Medicine and Biology, 2010. **37**(5): p. 547-555.
56. C. Rensch, A. Jackson, S. Lindner, R. Salvamoser, et al., *Microfluidics: A Groundbreaking Technology for PET Tracer Production?* Molecules, 2013. **18**(7): p. 7930-7956.
57. A.Y. Lebedev, *Microfluidic devices for radio chemical synthesis*, in *Microfluidic Devices for Biomedical Applications*, X. Li and Y. Zhou, Editors. 2013, p. 594-633.
58. C. Rensch, B. Waengler, A. Yaroshenko, V. Samper, et al., *Microfluidic reactor geometries for radiolysis reduction in radiopharmaceuticals.* Applied Radiation and Isotopes, 2012. **70**(8): p. 1691-1697.
59. C.K. Fredrickson and Z.H. Fan, *Macro-to-micro interfaces for microfluidic devices.* Lab on a Chip, 2004. **4**(6): p. 526-533.
60. G. Pascali, A. Berton, M. DeSimone, N. Wyatt, et al., *Hardware and software modifications on the Advion NanoTek microfluidic platform to extend flexibility for radiochemical synthesis.* Appl Radiat Isot, 2014. **84**: p. 40-7.
61. S.-A. Poulsen and R.J. Quinn, *Adenosine receptors: new opportunities for future drugs.* Bioorganic & Medicinal Chemistry, 1998. **6**(6): p. 619-641.
62. J. Linden, *Adenosine in Tissue Protection and Tissue Regeneration.* Molecular Pharmacology, 2005. **67**(5): p. 1385-1387.
63. B.B. Fredholm, A.P. IJzerman, K.A. Jacobson, K.-N. Klotz, et al., *International Union of Pharmacology. XXV. Nomenclature and Classification of Adenosine Receptors.* Pharmacological Reviews, 2001. **53**(4): p. 527-552.

64. Z.-L. Huang, Y. Urade, and O. Hayaishi, *The Role of Adenosine in the Regulation of Sleep.* Current Topics in Medicinal Chemistry, 2011. **11**(8): p. 1047-1057.
65. T.V. Dunwiddie and S.A. Masino, *The role and regulation of adenosine in the central nervous system.* Annu Rev Neurosci, 2001. **24**: p. 31-55.
66. K.A. Jacobson and Z.G. Gao, *Adenosine receptors as therapeutic targets.* Nat Rev Drug Discov, 2006. **5**(3): p. 247-64.
67. A.K. Dixon, A.K. Gubitz, D.J. Sirinathsinghji, P.J. Richardson, et al., *Tissue distribution of adenosine receptor mRNAs in the rat.* Br J Pharmacol, 1996. **118**(6): p. 1461-8.
68. A.-H. Li, S. Moro, N. Forsyth, N. Melman, et al., *Synthesis, CoMFA Analysis, and Receptor Docking of 3,5-Diacyl-2,4-Dialkylpyridine Derivatives as Selective A_3 Adenosine Receptor Antagonists.* Journal of Medicinal Chemistry, 1999. **42**(4): p. 706-721.
69. W. Wadsak, L.-K. Mien, K. Shanab, D.E. Ettlinger, et al., *Preparation and first evaluation of [^{18}F]FE@SUPPY: a new PET tracer for the adenosine A_3 receptor.* Nuclear Medicine and Biology, 2008. **35**(1): p. 61-66.
70. W. Wadsak, L.-K. Mien, K. Shanab, K. Weber, et al., *Radiosynthesis of the adenosine A3 receptor ligand 5-(2-[^{18}F]fluoroethyl) 2,4-diethyl-3-(ethylsulfanylcarbonyl)-6-phenylpyridine-5-carboxylate ([^{18}F]FE@SUPPY).* Radiochimica Acta, 2008. **96**(2): p. 119-124.
71. B.M. Liederer and R.T. Borchardt, *Enzymes involved in the bioconversion of ester-based prodrugs.* J Pharm Sci, 2006. **95**(6): p. 1177-95.
72. L. Azéma, C. Lherbet, C. Baudoin, and C. Blonski, *Cell permeation of a Trypanosoma brucei aldolase inhibitor: Evaluation of different enzyme-labile phosphate protecting groups.* Bioorganic & Medicinal Chemistry Letters, 2006. **16**(13): p. 3440-3443.
73. D. Haeusler, L. Nics, L.-K. Mien, J. Ungersboeck, et al., *[^{18}F]FE@SUPPY and [^{18}F]FE@SUPPY:2 — metabolic considerations.* Nuclear Medicine and Biology, 2010. **37**(4): p. 421-426.
74. H.H. Coenen, P.H. Elsinga, R. Iwata, M.R. Kilbourn, et al., *Fluorine-18 radiopharmaceuticals beyond [^{18}F]FDG for use in oncology and neurosciences.* Nuclear Medicine and Biology, 2010. **37**(7): p. 727-740.
75. P. He, S.J. Haswell, N. Pamme, and S.J. Archibald, *Advances in processes for PET radiotracer synthesis: Separation of [^{18}F]fluoride from enriched [^{18}O]water.* Applied Radiation and Isotopes, 2014. **91**(0): p. 64-70.
76. J.M. Gillies, C. Prenant, G.N. Chimon, G.J. Smethurst, et al., *Microfluidic technology for PET radiochemistry.* Appl Radiat Isot, 2006. **64**(3): p. 333-6.
77. K. Shanab, W. Wadsak, L.-K. Mien, M. Mitterhauser, et al., *Synthesis of in vivo Metabolites of the New Adenosine A_3 Receptor PET-Radiotracer [^{18}F]FE@SUPPY.* Heterocycles, 2008. **75**(2): p. 339-356.
78. R.C. Specht, *Interaction of Fluoride Ions and Ground Glass.* Analytical Chemistry, 1956. **28**(6): p. 1015-1017.
79. D.R. Burfield, K.-H. Lee, and R.H. Smithers, *Desiccant efficiency in solvent drying. A reappraisal by application of a novel method for solvent water assay.* The Journal of Organic Chemistry, 1977. **42**(18): p. 3060-3065.